Yuan et al. *Zool. Res.* 2023, 44(2): 303−314
https://doi.org/10.24272/j.issn.2095-8137.2022.384

ZR | Zoological Research

Article Open Access

A 1.1 Mb duplication CNV on chromosome 17 contributes to skeletal muscle development in Boer goats

Ying Yuan[1,2,#], Wei-Yi Zhang[1,2,#], Bai-Gao Yang[1,2], Dong-Ke Zhou[1,2], Lu Xu[1,2], Yong-Meng He[1,2], Hao-Yuan Zhang[1,2], Cheng-Li Liu[1,2], Yue-Hui Ma[3], Ming-Xing Chu[3], Wen-Guang Zhang[4], Hui-Jiang Gao[3], Lin Jiang[3], Fu-Ping Zhao[3], Lu-Pei Zhang[3], Ri-Su Na[4], Baatarchogt Oyungerel[5], Yan-Guo Han[1,2], Yan Zeng[1,2], Shi-Zhi Wang[1,2], Huai-Zhi Jiang[6], Hong-Ping Zhang[7], Xun-Ping Jiang[8], Jian-Ning He[9], Hao Liang[10], Kaushalendra Kaushalendra[11], Ya-Wang Sun[1,2], Yong-Fu Huang[1,2], Yong-Ju Zhao[1,2], Zhong-Quan Zhao[1,2], Guang-Xin E[1,2,*]

[1] *College of Animal Science and Technology*, *Southwest University*, *Chongqing* 400715, *China*
[2] *Chongqing Key Laboratory of Forage & Herbivore*, *Chongqing* 400715, *China*
[3] *Institute of Animal Science*, *Chinese Academy of Agricultural Sciences (CAAS)*, *Beijing* 100193, *China*
[4] *College of Animal Science*, *Inner Mongolia Agricultural University*, *Huhhot*, *Inner Mongolia* 010018, *China*
[5] *School of Animal Science & Biotechnology*, *Mongolian University of Life Sciences*, *Zaisan*, *Khan-uul*, *Ulaanbaatar* 17024, *Mongolia*
[6] *Animal Science and Technology College*, *Jilin Agriculture University*, *Changchun*, *Jilin* 130118, *China*
[7] *Farm Animal Genetic Resources Exploration and Innovation Key Laboratory of Sichuan Province*, *College of Animal Science and Technology*, *Sichuan Agricultural University*, *Chengdu*, *Sichuan* 611130, *China*
[8] *Key Lab of Agricultural Animal*, *Genetics*, *Breeding and Reproduction of Ministry of Education*, *College of Animal Science and Technology*, *Huazhong*, *Agricultural University*, *Wuhan*, *Hubei* 430070, *China*
[9] *College of Animal Science and Technology*, *Qingdao Agricultural University*, *Qingdao*, *Shandong* 266109, *China*
[10] *State Key Laboratory of Reproductive Regulation and Breeding of Grassland Livestock*, *School of Life Sciences*, *Inner Mongolia University*, *Hohhot*, *Inner Mongolia* 010070, *China*
[11] *Department of Zoology*, *Pachhunga University College*, *Mizoram University*, *Aizawl* 796001, *India*

ABSTRACT

The Boer goat is one of the top meat breeds in modern animal husbandry and has attracted widespread attention for its unique growth performance. However, the genetic basis of muscle development in the Boer goat remains obscure. In this study, we identified specific structural variants in the Boer goat based on genome-wide selection signals and analyzed the basis of the molecular heredity of related candidate genes in muscle development. A total of 9 959 autosomal copy number variations (CNVs) were identified through selection signal analysis in 127 goat genomes. Specifically, we confirmed that the highest signal CNV (HSV) was a chromosomal arrangement containing an approximately 1.11 Mb (CHIR17: 60062304–61171840 bp) duplicated fragment inserted in reverse orientation and a 5 362 bp deleted region (CHIR17:60145940–60151302 bp) with overlapping genes (e.g., *ARHGAP10*, *NR3C2*, *EDNRA*, *PRMT9*, and *TMEM184C*). The homozygous duplicated HSV genotype (+/+) was found in 96% of Boer goats but was not detected in Eurasian goats and was only detected in 4% of indigenous African goats. The expression network of three candidate genes (*ARHGAP10*, *NR3C2*, and *EDNRA*) regulating dose transcription was constructed by RNA sequencing. Results indicated that these genes were involved in the proliferation and differentiation of skeletal muscle satellite cells (SMSCs) and their overexpression significantly increased the expression of *SAA3*. The HSV of the Boer goat contributed to superior skeletal muscle growth via the dose effects of overlapping genes.

Keywords: Boer goat; CNV; Muscle development; SMSCs

INTRODUCTION

Boer goat is a world-renowned meat breed of goat characterized by a large body and good meat production. Because of its broad ecological adaptability, it has been widely introduced in many countries for the hybrid genetic improvement of native goats (Marques et al., 2021; Ncube

Received: 25 November 2022; Accepted: 06 February 2023; Online: 07 February 2023
Foundation items: This work was supported by the National Natural Science Foundation of China (32272834)
[#]Authors contributed equally to this work
*Corresponding author, E-mail: eguangxin@126.com

et al., 2022; Pérez-Baena et al., 2021). Many researchers have explored its meat quality (van Wyk et al., 2022), feeding mode (Pérez-Baena et al., 2021), and reproductive performance (Bezerra et al., 2019; Kholif et al., 2020), as well as the molecular basis of muscle development, coat color, and environmental adaptation (Chaosap et al., 2020; Shakweer & El-Rahman, 2020; Wang et al., 2019b; Xiong et al., 2020). However, the genetic basis for its superior muscle growth remains poorly understood.

Copy number variation (CNV) is a major form of genomic structural variation, defined as the deletion/duplication of genomic fragments of more than 1 kb caused by genome rearrangements (Xie & Tammi, 2009). CNVs participate in various biological functions and phenotype formation through the dosage effects of included genes and are involved in the reconstruction of gene regulatory regions (Pielberg et al., 2003; Shen et al., 2013; Xu et al., 2020). For example, *CCL3L1* copy exhibits a robust large-scale gene dosage effect on *CCL3L1* mRNA levels (Adewoye et al., 2018). The human *SLC2A3* gene locus located on chromosome 12p13.31 is unstable and prone to non-allelic homologous recombination events, generating multiple CNVs of *SLC2A3* that alter *SLC2A3* expression (Veal et al., 2014). Specifically, organ development, proliferation, and cellular degeneration are particularly susceptible to *SLC2A3* copy number alterations (Ziegler et al., 2020). Furthermore, the 16p11.2 and 22q11.2 genes involved in CNVs are thought to have copy number dose-dependent effects on the behavior of affected humans (Shishido et al., 2014). Overall, CNVs are closely related to the expression levels of the covered genes and the copy numbers of most genes are positively correlated with their expression (Shao et al., 2019). Recent studies have suggested that CNVs are key drivers of phenotypic diversity and economic traits in domesticated animals (Ladeira et al., 2022; Lye & Purugganan, 2019; Paudel et al., 2013), and are associated with goat muscle development (Huang et al., 2021; Liu et al., 2019).

Skeletal muscle is the main source of protein in edible meat (Yin et al., 2020), and its developmental status directly determines the growth-related economic traits of animals (Dodson et al., 2010). The formation of new muscle fibers in skeletal muscle depends on the activation of muscle-specific precursor cells (Dumont et al., 2015; Relaix & Zammit, 2012). The self-renewal and proliferation of skeletal muscle satellite cells (SMSCs) can provide many myogenic cells, which redifferentiate into myoblasts and fuse into myotubes to form new muscle fibers (Chang & Rudnicki, 2014).

The development of SMSCs is a complex process due to the co-regulation of numerous signaling pathways and genes (Giordani et al., 2018; Milewska et al., 2014). In recent decades, the genetic basis of goat skeletal muscle development has been investigated. Studies have shown that the *MSTN* gene is a negative regulator of skeletal muscle growth and development and functions by controlling the number, size, and type of muscle fibers (Bi et al., 2021). *GSK3β* regulates the expression of the *MYHC-2A* gene via *NFATC2* to promote SMSC differentiation in goats (Wang et al., 2019a). The mTOR signaling pathway regulates the phosphorylation of myocyte enhancer factor 2 (*MEF2*) through *ILK*, thereby affecting SMSC proliferation and differentiation (Wu et al., 2015).

In this study, we aimed to identify CNVs and high-frequency dominant genotypes associated with the extraordinary economic phenotypes in Australian Boer goats via genome-wide selection signal analysis. We also clarified the molecular roles of candidate genes carried by the variants in the proliferation and differentiation of SMSCs and the dose effect-based expression regulation of downstream genes.

MATERIALS AND METHODS

Genome-wide sequencing and selection signal analysis of CNV dataset

All applicable international, national, and institutional guidelines for the care and use of animals were strictly followed. All animal collection protocols complied with the current laws of China. The experimental protocols were approved by the Animal Care Committee of Southwest University (Permit No. IACUC-20210415-04) in compliance with the recommendations of the Regulations for the Administration of Affairs Concerning Experimental Animals of China.

A total of 127 publicly available goat genome datasets were downloaded from the NCBI Sequence Read Archive (SRA), including 46 Australian Boer goats from our previous study (Yang et al., 2021) and 81 other goats (45 African, 16 European, and 20 Asian goats) as the control group (Supplementary Table S1).

The raw genomic data were trimmed and filtered using Trimmomatic software (v0.36). High-quality clean reads were mapped to the goat reference genome (ARS1, GCF_001704415.1) using BWA-MEM (v0.7.17-r1188) with default parameters. Potential polymerase chain reaction (PCR) duplicates were removed by Picard (http://broadinstitute.github.io/picard). CNVcaller (Wang et al., 2017b) was used to determine CNVs, retaining those with silhouette score>0.65 and minor allelic frequency (MAF)>0.05 to prevent possible false positives. Selective sweep analysis of CNVs was performed with V_{ST} and F_{ST}. Variants were annotated by ANNOVAR (ANNOate VARiation). Candidate genes were identified and annotated from the top 20 CNVs using the V_{ST} and F_{ST} indices. Candidate genes were also annotated based on Gene Ontology (GO) and Kyoto Encyclopedia of Genes and Genomes (KEGG) analyses using the online tool KOBAS (http://kobas.cbi.pku.edu.cn/kobas3) with corrected P<0.05 as the threshold for significant enrichment.

To further explore the genotype frequencies of key candidate CNVs in Chinese indigenous goat populations, we followed the above-mentioned CNV identification methods to supplement the CNV genotypes of four indigenous breeds in southwest China (20 Dazu black goats, 20 Youzhou black goats, 20 Hechuan white goats, and 20 Hainan goats) (Supplementary Table S2). Venous blood samples (1.5 mL) were collected, and genomic DNA was extracted using a DNeasy Blood & Tissue Kit (Qiagen, Germany). DNA libraries were constructed with an Illumina NGS Fast DNA Library Prep Set Illumina Kit (Illumina, USA). The genome of each animal was sequenced using the Illumina NovaSeq 6000 system for 10× sequencing (BGI, China). All bioinformatics analysis steps were performed as described above.

Exploration of candidate CNV structures using long-read genome-wide sequencing and PCR-Sanger sequencing

One DNA sample was collected from each of the 46 Australian Boer goats. A SMRT bell CLR library was constructed using a Pacific Biosciences SMRTbell Express Template Prep Kit 2.0.

The constructed libraries were size-selected on a BluePippin™ system for molecules ≥25 kb and subjected to primer annealing. The SMRTbell templates were bound to polymerases using a DNA/Polymerase Binding Kit. Sequencing was carried out using the Pacific Bioscience Sequel platform (PacBio, USA).

To verify the structural variant genotypes of chromosomal rearrangements, PCR primers (Supplementary Table S3) targeting breakpoints based on an approximately 1.11 Mb chromosomal rearrangement (CHIR17:60062304–61171840) were designed using the Primer (v3.04) online tool (http://bioinfo.ut.ee/primer3-0.4.0/). For PCR amplification, 2×TransTaq® High Fidelity (HiFi) PCR SuperMix II (TransGen Biotech, China) was used. The PCR conditions consisted of initial denaturation at 94 °C for 5 min, followed by 35 cycles of denaturation at 94 °C for 30 s, annealing at locus-specific annealing temperature (Tm) for 30 s, and extension at 72 °C for 2 min, with a final extension at 72 °C for 7 min. Sanger sequencing was conducted using two methods on the ABI 3730 sequencing platform (Life Technologies, USA).

Culture and identification of SMSCs in goats

First, 3 cm^3 leg muscle samples were obtained from 1-month-old Dazu black goats. After removing fat and connective tissues, the muscles were digested with 0.1% type I collagenase (Solarbio, China) and 0.25% trypsin (HyClone, USA) to release the cells. The SMSC suspension was filtered and detached, after which the cells were cultured 10% growth medium (GM) containing Dulbecco's Modified Eagle Medium (DMEM/F; Thermo Fisher Scientific, China), 10% fetal bovine serum (Thermo Fisher Scientific, China), and 2% penicillin/streptomycin (Invitrogen, USA) at 37 °C in a humidified atmosphere of 5% CO_2. Differentiated SMSCs were induced using differentiation medium (DM) containing DMEM and 2% horse serum (HyClone, USA) when their density reached 70%–80% in the GM. Immunofluorescence staining of Pax7 was performed to identify SMSC purity (Feng et al., 2018), and Pax7 monoclonal rabbit antibodies were provided by Absin (China).

Candidate gene overexpression vector construction and transfection into SMSCs

To identify effects on SMSC proliferation and differentiation, lentiviral vectors (HBLV-*ARHGAP10*-3xflag-ZsGreen-PUR, HBLV-*EDNRA*-HIS-mCherry-BSD, and HBLV-*NR3C2*-3xflag-ZsGreen-PURO; HANBIO, China) expressing flag-tagged *ARHGAP10* (Gene ID: 102173323), *EDNRA* (Gene ID: 102174144), and *NR3C2* (Gene ID: 102172834) were first constructed. Their cDNAs were synthesized by PCR amplification with corresponding primer pairs (Supplementary Table S4) and inserted between the EcoRI and BamHI sites. HBLV-ZsGreen-PURO and HBLV-mCherry-BSD empty vectors were used as negative controls. Lentiviral transfection was performed when SMSC density reached 60%–70%. Transfection efficiency was assessed based on cell fluorescence using a fluorescence microscope (Leica DMi8, Germany) after 48 h.

At 12, 24, 36, and 72 h after transfection of overexpressed candidate genes into the SMSCs, cell proliferation was measured using a CCK8 Kit (Solarbio, China) by recording absorbance at 450 nm and running three parallel replicates. At 48 h after transfection, an EdU (5-ethynyl-2'-deoxyuridine) experiment was performed using a C10310 EdU Apollo *In Vitro* Imaging Kit (Ribobio, China). At least four fields were randomly selected to observe the number of stained cells under a fluorescence microscope (Leica DMi8, Germany).

To identify SMSC differentiation when candidate genes were overexpressed, we carried out lentiviral transfection, followed by cell culture for 36 h at 37 °C. SMSC differentiation was induced for 4 days by switching from GM to DM. Total RNA was extracted using RNAiso Plus (Solarbio, China). The mRNA expression levels of myogenic differentiation marker genes (*MyoD*, *MyoG*) were measured by quantitative real-time PCR (qRT-PCR) (Metzger et al., 2020).

Molecular regulatory network investigation of overexpressed candidate genes in SMSCs by RNA sequencing (RNA-seq)

The SMSC sample settings for RNA-seq were: *ARHGAP10* overexpressed group (AA) and its no-load control (AO); *EDNRA* overexpression group (EA) and its no-load control (EO); and *NR3C2* overexpression group (NA) and its no-load control (NO). Three biological replicates were established for each group. Total RNA was extracted using a Trizol Reagent Kit (Invitrogen, USA). RNA quality was assessed with an Agilent 2100 Bioanalyzer (Agilent Technologies, USA). RNA-seq cDNA libraries were constructed using a NEBNext Ultra RNA Library Prep Kit (NEB #7530, New England Biolabs, USA). Sequencing was performed on the Illumina NovaSeq 6000 system (BGI, China).

Fastp (v0.18.0) was used to filter raw data (PRJNA843937) to obtain clean reads. The short-read alignment tool Bowtie2 (v2.2.8) was used to map the reads to the ribosomal RNA (rRNA) database. The rRNA-mapped reads were then removed. Paired-end clean reads were mapped to the reference genome (ARS1, GCA_001704415.1) using HISAT (v2.2.4) with default parameters. The mapped reads of each group were assembled using StringTie (v1.3.1) in a reference-based approach. For each transcription region, fragments per kilobase of transcripts per million mapped reads (FPKM) values were calculated to quantify expression abundance using RSEM software (Li & Dewey, 2011). Differential gene expression was analyzed by DESeq2 (Love et al., 2014). Genes with a false discovery rate (FDR)<0.05 and absolute fold-change≥2 were considered as significant differentially expressed genes (DEGs).

Bioinformatics analysis accuracy based on RNA-seq data was verified using a CFX96-Touch™ Real-Time PCR Detection system (Bio-Rad, USA). All RNA samples used for qRT-PCR were the same as those used for RNA-seq. The cDNA was synthesized using a First-Strand cDNA Synthesis Kit (Takara Bio, RR047A, China). Primer Premier 6 (Premier Biosoft, USA) was used to design the primers for the genes (Supplementary Table S5).

For qRT-PCR amplification, in accordance with the manufacturer's instructions, the reaction volume (20 μL) contained 10 μL of 2×SYBR Green PCR Master Mix (Takara Bio, China), 20 ng of cDNA, 0.5 μL (10 mmol/L) of each primer, and ddH_2O to the final volume. The qRT-PCR amplification system included: one cycle at 95 °C for 3 min, followed by 40 cycles at 95 °C for 10 s and 55 °C for 30 s. Within the runs, the samples were assayed in triplicate, and the maximum acceptable standard deviation of the threshold cycle (CT) was 0.2. Each qRT-PCR run was repeated at least three times. Glyceraldehyde 3-phosphate dehydrogenase (*GAPDH*) was used to normalize gene expression (reference gene). The relative expression levels of different qRT-PCR data were analyzed using the $2^{-\Delta\Delta Ct}$ method (Livak &

Schmittgen, 2001). Statistical analysis of relative mRNA expression was carried out using SPSS v19.0 (SPSS, USA).

RESULTS

Genome-wide selection signal analysis of CNVs in Boer goat

In this study, 9 959 CNVs were obtained on the autosomes of 127 goats. Twenty overlapping CNVs were screened according to the top 1% selection signals of the two parameters (F_{ST}≥0.430998, V_{ST}≥0.597069727; Figure 1A). A total of 23 candidate genes (e.g., *EDNRA*, *CYBA*, and *PBRM1*) were identified from those CNVs (Supplementary Table S6).

Eleven of the 23 candidate genes were enriched in 33 KEGG signaling pathways (Figure 1B; Supplementary Table S7), including growth and development-related pathways (such as osteoclast differentiation (*CYBA*)), metabolism-related signaling pathways (inositol phosphate metabolism (*PLCH2*) and metabolic pathways (*PLCH2*, *NDST3*, and *MVD*)), and biological regulatory function-related signaling pathways (MAPK signaling pathway (*CACNA1B*)). Moreover, 21 of the candidate genes were enriched to 238 GO terms (Figure 1C; Supplementary Table S8), of which 56 were significantly enriched (corrected P<0.05). According to the classification results, three GO terms were related to muscle contraction function, including artery smooth muscle contraction (*EDNRA*), smooth muscle contraction (*EDNRA*), and positive regulation of smooth muscle cell proliferation (*CYBA*). Some GO terms related to growth and development were also enriched, such as positive regulation of endothelial cell proliferation (*CYBA*), neural crest cell development (*EDNRA*), and mitotic cell cycle (*PBRM1*). Other GO terms were related to immune function (positive regulation of phagocytosis (*CYBA*)) and reproduction (oogenesis (*KMT2D*) and *in utero* embryonic development (*EDNRA*)).

Precise structure of key candidate CNVs in Boer goats

The two CNVs with the highest signal values (CNV1: F_{ST}=0.918858, V_{ST}=0.855420854, CHIR17:60062001–60297500 bp; CNV2: F_{ST}=0.918858, V_{ST}=0.877347065, CHIR17:60301001–61018500 bp) contained five coding genes (*ARHGAP10*, *NR3C2*, *EDNRA*, *TMEM184C*, and *PRMT9*). The full length of the duplication CNVs (CNV1 and CNV2) on CHIR17 was approximately 1.11 Mb, as determined by the Integrative Genome Viewer (IGV) with short reads. We confirmed that the two CNVs were seamlessly unified (HSV; Figure 2A), that is, they did not include at 4 145 bp spacer sequence, as determined by long-read and PCR-Sanger sequencing of homozygous individuals. Average read coverage of the different HSV genotypes (Figure 2B) and frequency of the HSV genotypes within populations located in different geographic areas were determined. The homozygous duplication (+/+) genotype was found in 96% of the Boer goats, 4% of the indigenous African goats, and none of the Eurasian goats (Figure 2C).

Long reads sequenced from a homozygous individual with HSV (+/+) were used for HSV structural analysis. First, a 5 363 bp (CHIR17:60145940–60151302 bp) region was observed within the 1.11 Mb HSV region of the homozygous HSV (+/+) individual without an extra copy (Figure 2D). In addition, many reads mapped to the two edges of the HSV were reverse-mapped to the outer edges of the region (CHIR17:60145940–60151302 bp), as observed by IGV. In detail, more than 80% of reads mapped to CHIR17:60137768–60145940 bp were also reversely located in the CHIR17:61167664–61171840 region (Figure 2D), and a high frequency of reads were mapped to both CHIR17:60062304–60063156 and CHIR17:60151302–60153676 in opposite

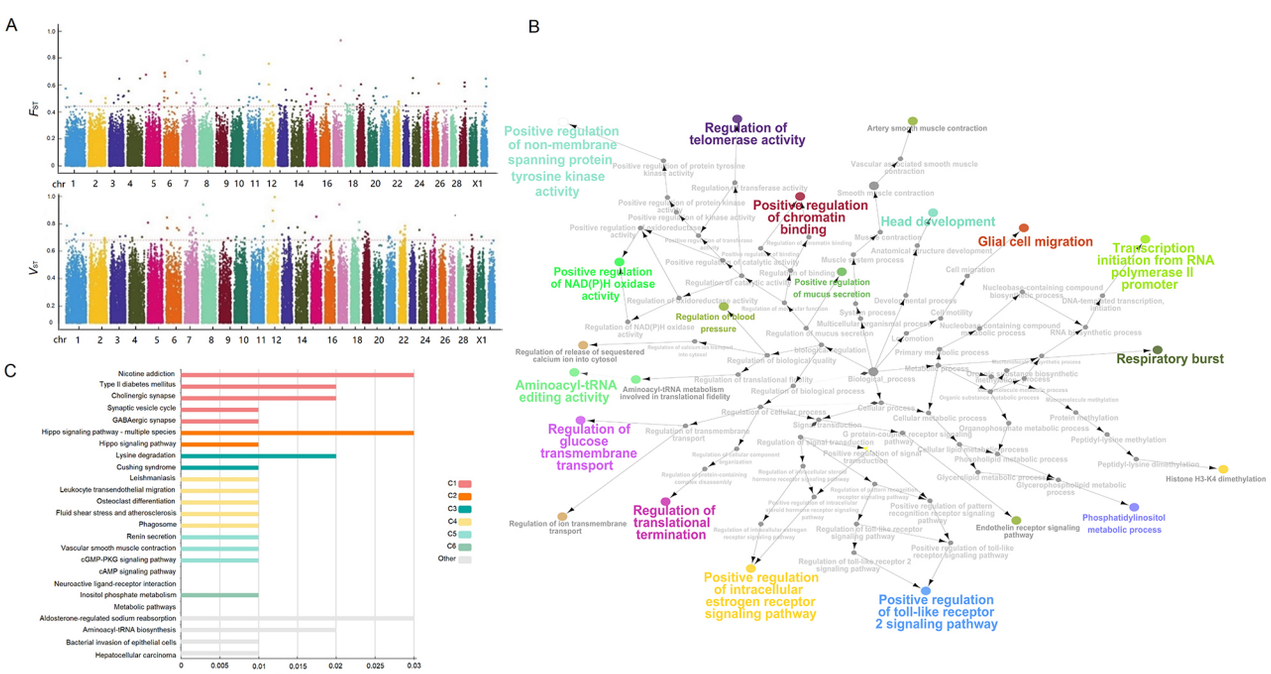

Figure 1 Genome-wide selective sweep analysis of Boer goats based on CNVs

A: Manhattan plot of F_{ST} and V_{ST} showing CNV-based selection signals of 46 Boer goats in comparison to 81 non-meat goats and top 1% of intersections of sweep windows between F_{ST} and V_{ST}. B: KEGG pathways enriched in 11 candidate genes, with top 20 intersections of selection signal parameters. C: GO network enriched in 21 candidate genes, with top 20 overlapping CNVs of two selection signal parameters. Different colors represent different biological function classifications, and size is determined by amount of GO enrichment.

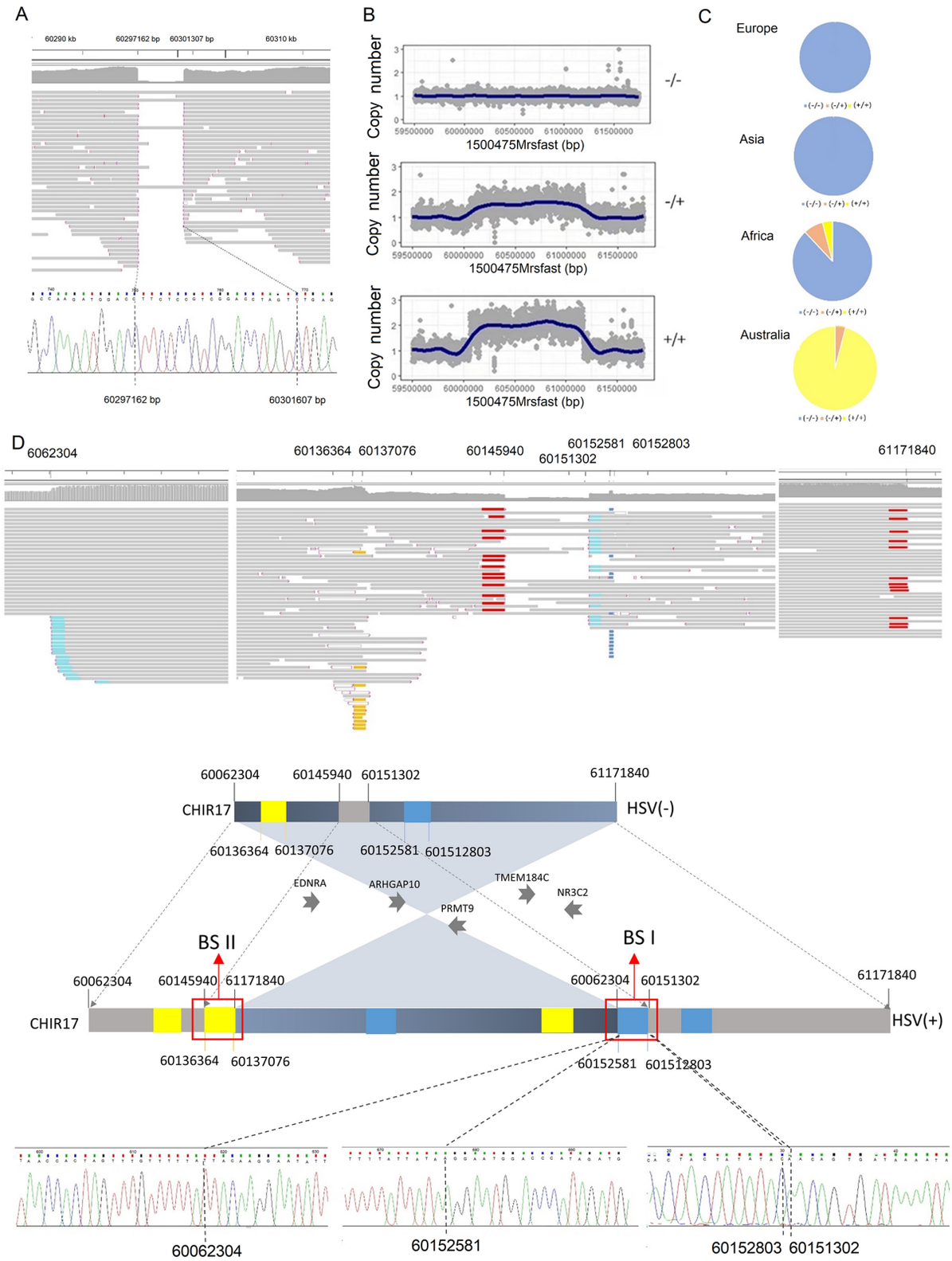

Figure 2 Genomic structure of HSV on CHIR17 in goats

A: IGV screenshots of Nanopore long-read sequences, showing lack of the 4 145 bp spacer sequence between CNV1 and CNV2, as determined by long-read and PCR-Sanger sequencing of homozygous goats. B: Coverage of genomic reads of different genotypes of HSV. C: Genotype frequency distribution of homozygous duplicated HSV (+/+) in different geographical populations. D: Close-ups of IGV screenshots of Illumina long-read sequences, illustrating duplication of CHIR17 at the boundaries of the variant sites. Red and green reads are mapped at different locations. Extremely prominent multicopy elements (MCE1, MCE2) are in yellow and blue. E: Schematic of variant on CHIR17, showing inversely inserted ~1.1 Mb segment and deleted 5 363 bp region (CHIR17:60145940–60151302 bp) by retrovirus direction; location and orientation of annotated genes and loci in involved genome regions are shown. F: Experimental confirmation of complex structural variant. Sanger sequencing of PCR products of variant allele precisely defines breakpoints of fusion of CHIR17 segments.

directions (Figure 2D). Therefore, we initially assumed that the chromosomal rearrangement structure of the HSV was formed by the insertion of the extra 1.11 Mb duplication in the reverse orientation and by the deletion of the ~5.3 kb region (Figure 2E). Here, the two end sequences of the HSV reverse insertion sites were named boundary sequence I (BS I, CHIR17: 60062304 bp) and boundary sequence II (BS II, CHIR17:61171840 bp). We designed primers extending approximately 1 kb on each side of BS I, which were then verified by PCR-Sanger sequencing. The product sequence results are shown in Figure 2F. The primers designed at each 1 kb extension of BS II and PCR amplification were unsuccessful and accurate sequence assignments were not obtained due to deficiencies in the reference genome assembly.

Two extremely prominent multicopy elements (MCEs) were widely observed in the HSV region (Figure 2D), including MCE1 (718 bp in size, mapped to CHIR17:60136360–60137078 bp) and MCE2 (222 bp in size, mapped to CHIR17:60152581–60152803 bp). Some duplicate reads of both elements were also positioned adjacent to BS I (Supplementary Figure S1) and BS II (Supplementary Figure S2). Although a nucleic acid BLAST search of the NCBI database did not retrieve any information on MCE2, MCE1 showed 96.6% similarity to *Babesia ovata* Retrovirus-related Pol poly LINE-1 (XM_029013938.1).

Cell culture, identification, and transfection

According to the KEGG results of the five genes within the 1.11 Mb duplicated region, only three were enriched in KEGG pathways related to bacterial invasion of epithelial cells (*ARHGAP10*), vascular smooth muscle contraction (*EDNRA*), and aldosterone-regulated sodium reabsorption (*NR3C2*).

The isolated and cultured SMSCs were identified by immunofluorescence (Wang et al., 2020). Results showed that the expression efficiency of Pax7 was 82.3% (Supplementary Figure S3A). Infection efficiency was assessed using different multiplicities of infection (MOIs: 30, 60, 90, and 120) (Supplementary Figure S4). At an MOI of 90, the fluorescence intensity was highest and SMSCs grew well (Supplementary Figure S3B). At 48 h after lentiviral transfection, the gene expression levels of *ARHGAP10*, *NR3C2*, and *EDNRA* were significantly higher than those in the control group (P<0.01; Supplementary Figure S3C).

Involvement of overexpressed candidate genes (*ARHGAP10*, *NR3C2*, and *EDNRA*) in proliferation and differentiation of SMSCs

The effects of the three candidate genes on SMSC proliferation were determined by the CCK-8 method. Cells proliferated rapidly within 24–36 h after lentiviral transfection, and the proliferation rate of SMSCs transfected with *ARHGAP10* and *NR3C2* overexpressing lentiviruses was significantly higher than that of the control cells (Figure 3C). We also examined the proliferation of SMSCs by EdU assay and found that *ARHGAP10* and *NR3C2* overexpression significantly increased the number of EdU-positive cells in the proliferation phase (Figure 3A, B).

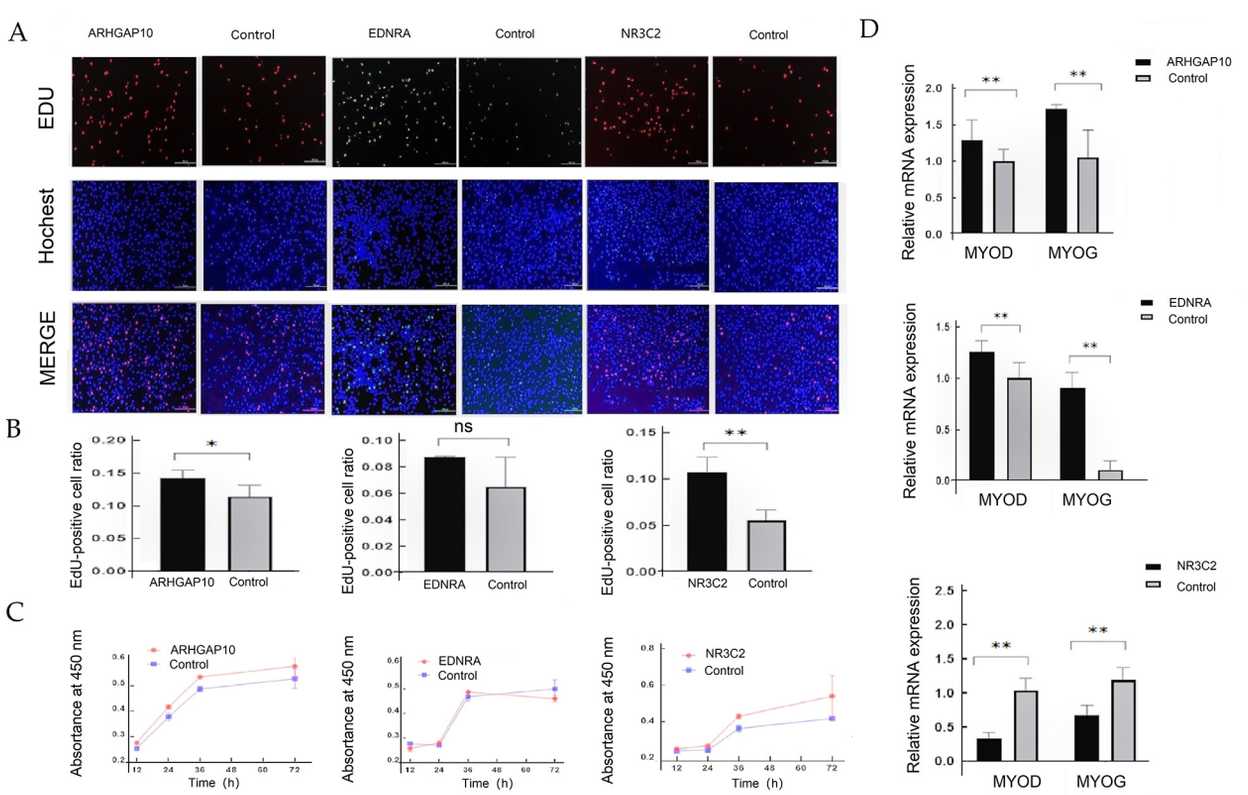

Figure 3 Effects of overexpression of *ARHGAP10*, *NR3C2*, and *EDNRA* or control on SMSC proliferation and differentiation

A: EdU assay results for SMSCs after overexpression of *ARHGAP10*, *NR3C2*, and *EDNRA* for 48 h, where EdU (red) fluorescence indicates proliferation and Hoechst (blue) fluorescence indicates nuclei. B: EdU-positive cell ratio of SMSCs after overexpression of *ARHGAP10*, *NR3C2*, and *EDNRA* for 48 h. Data are mean±standard error of the mean (*SEM*) (n=6). C: Cell growth curves of SMSCs measured by CCK-8 Kit after overexpression. D: Effects of mRNA expression of *MyHC*, *MyoD*, and *MyoG* in overexpressed *ARHGAP10*, *NR3C2*, and *EDNRA* genes on SMSC differentiation. ns: No significance; *: P<0.05; **: P<0.01 vs. Control.

The differentiation effects observed after SMSCs were induced to differentiate for 4 days is shown in Supplementary Figure S5. Analysis of the effects of candidate gene overexpression on SMSC differentiation revealed that the relative mRNA expression levels of differentiation marker genes (*MyoD* and *MyoG*) increased after transfection with *ARHGAP10*- and *EDNRA*-carrying lentiviruses (Figure 3D). In contrast, the relative mRNA expression levels of *MyoD* and *MyoG* were inhibited in SMSCs after *NR3C2* transfection.

Molecular heredity regulation basis of overexpressed candidate genes in SMSCs

To further understand the regulatory mechanism of the *ARHGAP10*, *NR3C2*, and *EDNRA* genes in goat SMSCs, we performed RNA-seq of the transfected SMSCs and identified changes in related genes during cell proliferation and differentiation. A total of 273 significant DEGs were identified in the NA versus NO group, including 228 up-regulated genes (e.g., *BMP2*, *MYH3*, and *MYORG*) and 45 down-regulated genes (e.g., *EGR3*, *HAS2*, and *LIF*) (Figure 4A). Five significant DEGs (*CFB*, *C2*, *CYP26B1*, *SLC7A8*, and *SLPI*) were identified in the EA versus EO group, all of which were significantly up-regulated. One significant DEG (*SAA3*) was identified in the AA versus AO group, which was significantly up-regulated.

In the NA versus NO group, 125 DEGs were enriched in 223 pathways (Figure 4B), including several well-known pathways involved in cell growth and muscle development, such as the calcium signaling pathway, cyclic guanosine monophosphate-dependent protein kinase G (cGMP-PKG) signaling pathway, and transforming growth factor (TGF) signaling pathway. Many DEGs (e.g., *TGF-B2*, *MYH3*, *ANKRD1*, and *MYH15*) were involved in growth and development (Figure 4C), including muscle cell differentiation (e.g., muscle cell differentiation and cardiac muscle cell cycle based on GO annotation).

We also explored mRNA expression of DEGs in the NA versus NO group (Figure 5A) and EA versus EO group (Figure 5B). Notably, mRNA expression of *SAA3* was up-regulated in the SMSCs after overexpression of *ARHGAP10*, *EDNRA*, and *NR3C2* (Figure 5C). DEG validation by qRT-PCR was consistent with the RNA-seq results, confirming the stability and reliability of the transcriptome data in this study.

DISCUSSION

In this study, Australian Boer goats were shown to carry a high frequency of a homozygous-duplicated genotype of HSV. This duplicated genotype was not found in indigenous European and Asian goats but was detected at a low frequency in indigenous African goats. This finding suggests that this duplicated genotype may have originated from Africa, as Boer goats were initially bred by crossing indigenous African goats with European goats (Malan, 2000).

A large number of chromosomal rearrangements are distributed within vertebrate genomes (Tsai & Lieber, 2010), which are involved in a wide variety of biological functions and the formation of various phenotypes (Castronovo et al., 2015; Kot et al., 2021). A potential lentiviral transposable sequence appeared at junctional boundaries formed by the HSV chromosomal rearrangements. Various studies have shown that repetitive sequence elements of retroviruses may lead to large-scale chromosomal deletions, duplications, and rearrangements via homologous recombination (Hughes & Coffin, 2001). Evidence suggests that the frequency of rearrangements is higher when the LINE-1 copy number within the genomic region is high (Kemp & Longworth, 2015). Hence, HSV may be a retrovirus-directed chromosomal rearrangement.

Several studies have demonstrated that CNVs can promote phenotypic variation through dosage effects on gene expression (Berkel & Cacan, 2022; Pielberg et al., 2003). Evidence also suggests that the three genes within HSV identified in our study are involved in the development of

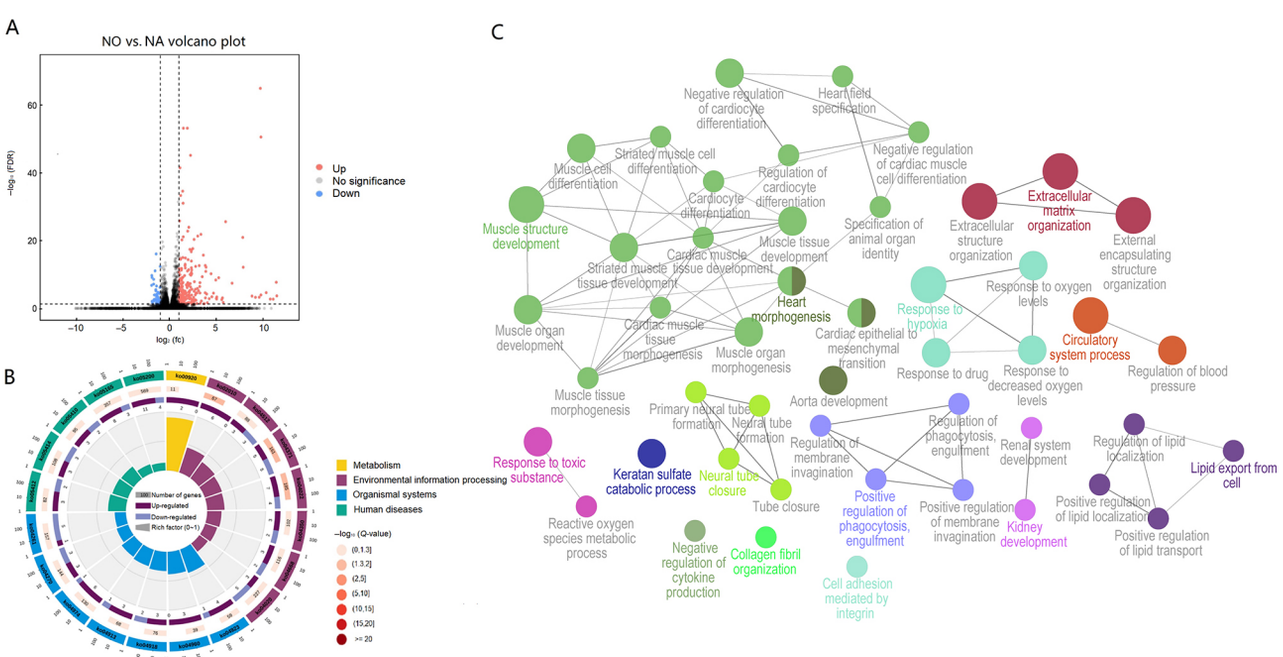

Figure 4 Transcriptomic changes in SMSCs after *NR3C2* overexpression

A: Volcano plot clustering of DEGs in samples transfected with overexpressed *NR3C2*. B: Pathways of DEGs in NA versus NO group according to KEGG enrichment analysis. C: Network diagram of GO terms enriched in DEGs in NA vs. NO group.

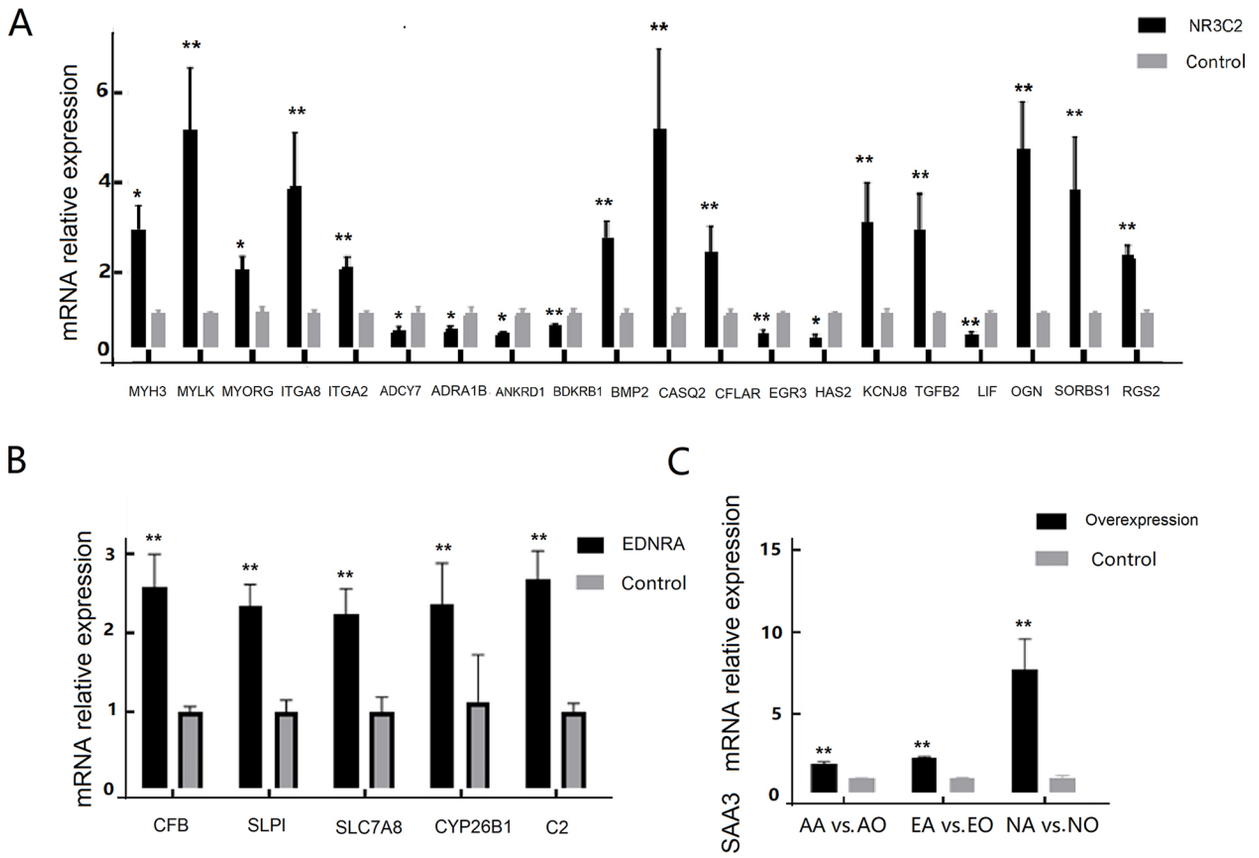

Figure 5 Results of mRNA expression of DEGs

A: mRNA expression of DEGs involved in muscle development in samples transfected with overexpressed *NR3C2* or control. B: mRNA expression of DEGs in samples transfected with overexpressed *EDNRA* or control. C: mRNA expression of *SAA3* in SMSCs after overexpression of *ARHGAP10*, *EDNRA*, and *NR3C2*. Data are mean±*SEM* (*n*=6). *: *P*<0.05; **: *P*<0.01 vs. control.

muscle cells. For example, Rho GTPase activating protein 10 (*ARHGAP10*) not only regulates the Rho-GTPase signaling pathway associated with actin cytoskeleton dynamics and cell proliferation and differentiation by encoding a potential cytoskeletal Rho-GTPase-activating protein but is also highly expressed in muscles and involved in cell differentiation (Bassères et al., 2002; Shibata et al., 2001). Coincidentally, *ARHGAP10* is reported to be involved in the formation of intramuscular fat in Japanese black cattle (Ueda et al., 2021). Nuclear receptor subfamily 3 group C member 2 (*NR3C2*) is a key component of hypothalamic-pituitary-adrenal neuroendocrine axis regulation, and variants in this gene are associated with muscle glycogen content and meat quality traits in male Nellore cattle (Poleti et al., 2015). *NR3C2* also contributes to muscular dystrophy relief and skeletal muscle repair in acute muscle injury (Howard et al., 2022). Endothelin receptor type A (*EDNRA*) is involved in various physiological functions, including smooth muscle contraction and fetal muscle development (Kobayashi et al., 2016; Sato et al., 2008).

The development of skeletal muscles is determined by the co-regulation of multiple signaling pathways, such as the adherens junction and Ca^{+} signaling pathways (Su et al., 2018). In addition, mTOR plays an essential role in satellite cell function and skeletal muscle regeneration by controlling the expression of myogenic genes (Zhang et al., 2015), while WNT is involved in myogenesis, neuromuscular synapses, and fibrosis (Cisternas et al., 2014). Specifically, activation of the TNF, MAPK/ERK, and PI3K/Akt pathways promotes proliferation and differentiation of adult muscle cells (Elia et al., 2007). Furthermore, the DNA methylation status of Wnt and TGF-β signaling is a key factor regulating SMSC development and function (Zhang et al., 2019). Here, many of the above-mentioned pathways were enriched in DEGs according to the NA versus NO RNA-seq results, indicating that *NR3C2* is involved in the signal transduction of many regulatory pathways related to skeletal muscle development.

Muscle satellite cells play a critical role in muscle growth via activation of the cell cycle in quiescent satellite cells (Chang & Rudnicki, 2014). Based on GO analysis, many DEGs from the NA versus NO RNA-seq group were associated with the cell cycle. For example, up-regulation of interferon regulatory factor 1 (*IRF1*) can accelerate cell cycle progression (Zhang et al., 2013), and growth arrest and DNA damage-inducible gene gamma (*GADD45G*) is associated with cell cycle checkpoints, apoptosis, and DNA repair (Humayun & Fornace, 2022). The centrosome scaffold protein (CEP192) recruits mitotic protein kinases Aurora A and PLK1 to the centrosome, and is essential for bipolar spindle assembly with centrioles to promote bipolar spindle formation and cell cycle regulation (Chinen et al., 2021; Nasa et al., 2017). Up-regulation of the adenosine triphosphate-binding cassette subfamily B member 1 (*ABCB1*) can reduce cell viability, promote apoptosis, and induce cell cycle arrest in G2/M (Zhou et al., 2019).

Satellite cell activation is accompanied by extensive cell migration (Yin et al., 2013). Our GO analysis results confirmed that DEGs from the NA versus NO RNA-seq group were involved in cell migration and positive regulation. For example,

as an important cytoskeletal protein, NEDD9 regulates cell proliferation, migration, invasion, and survival (Wang et al., 2017a). Bradykinin receptor B1 (*BDKRB1*) is a specific regulator of immune cell entry into the central nervous system and regulates lymphocyte migration across the blood-brain barrier endothelium *in vitro* (Schulze-Topphoff et al., 2009). Bradykinin expression can also induce the migration and invasion of glioma cells through *BDKRB1*-mediated calcium influx and subsequent behavior (Sun et al., 2020).

Complete skeletal muscle growth and repair includes SMSC growth and proliferation, myotube fusion, and myoblast production (Delaney et al., 2017). Here, many DEGs identified in the NA versus NO RNA-seq group were involved in these biological processes. In particular, functional loosening of cadherin 1 (*CDH1*) can promote and prevent quiescent SMSCs from switching on the cell cycle and ultimately compensates for the proliferation of muscle precursor cells (Christensen et al., 2007). Overexpression of CASP8 and FADD-like apoptosis regulator (*CFLAR*), also known as *c-FLIP*, can induce nuclear factor-κB (NF-κB) activation and promote SMSC proliferation (Giampietri et al., 2010). Early growth response 3 (*EGR3*), a zinc finger transcription factor, regulates diverse cellular functions and is involved in muscle cell proliferation (Kurosaka et al., 2017). Reduced *EGR3* expression is associated with attenuated function of SMSCs and hinders muscle cell regeneration in aged individuals (Ogura et al., 2020). Ankyrin repeat domain protein 1 (ANKRD1) is a transcriptional co-regulator in striated muscles and is involved in myofibril assembly (Boskovic et al., 2018). Skeletal muscle regeneration is also controlled by various extracellular factors, such as *TGF-β2*, which encodes transforming growth factor β2; this protein regulates skeletal muscle growth, stimulates SMSC proliferation, and restores muscle regeneration potential by perturbing β-catenin in SMSCs (Rudolf et al., 2016). In addition, fatty acid translocase cluster of differentiation (*CD36*) is not only related to the binding and transport of long-chain fatty acids but is also involved in fatty acid metabolism in skeletal muscles (Ibrahimi et al., 1999). Studies have reported that *CD36* deficiency impairs SMSC function and delays muscle regeneration (Verpoorten et al., 2020).

Six DEGs were identified in the EA versus EO RNA-seq group, which are widely involved in biological processes, such as growth and immunity. Cytochrome P450 family 26 subfamily B member 1 (*CYP26B1*) can regulate tongue muscle differentiation via retinoic acid signaling (Okano et al., 2008). *CYP26B1* also promotes maxillary tendon condensation and musculoskeletal patterning in zebrafish embryos (McGurk et al., 2017). Complement factor B (*CFB*) is involved in an alternative pathway of complement expression in muscle cells *in vitro*, with evidence showing that local complement expression in skeletal muscles is associated with certain muscle inflammatory or pathological processes *in vivo* (Legoedec et al., 1995). *SLC7A8* expression impairs proteolysis and affects carcass characteristics and meat quality in yak (Liu et al., 2021). Finally, secretory leukoprotease inhibitor (*SLPI*) can suppress proinflammatory cytokine production in lipopolysaccharide-stimulated cells, prevent neutrophil infiltration in mouse models of lung and liver injury, and modulate activity of transcription factor NF-κB (Douglas & Hannila, 2022).

This study showed that overexpression of all candidate genes significantly up-regulated the transcriptional expression of serum amyloid antigen 3 (*SAA3*). Abnormal local inflammatory signaling of skeletal muscles is considered a contributing factor in sarcopenia (Buford et al., 2009). The *SAA* family, consisting of major vertebrate acute-phase reactants, plays an important role in host defense during inflammation (Uhlar & Whitehead, 1999). *SAA3* is associated with obesity and insulin resistance in humans (Scheja et al., 2008). Specifically, *SAA3* levels show a positive correlation with obesity (Ji et al., 2022). Furthermore, *Lycium barbarum* polysaccharide can improve diabetes by inhibiting the effects of NF-κB activation in mouse models of diabetic nephropathy to reduce *SAA3* expression (Wan et al., 2022). In addition, studies have reported that *SAA3* is required for normal weight and immunometabolic function of *SLC2A3* in mice (Ather & Poynter, 2018).

CONCLUSIONS

The proliferation and differentiation of SMSCs play an important role in muscle development. Our study first identified the complex structure of a high frequency 1.1 Mb duplication CNV in Boer goats and clarified that a dosage effect on the expression of overlapping genes (*ARHGAP10*, *NR3C2*, and *EDNRA*) significantly contributed to SMSC proliferation and differentiation. This study not only improves our understanding of the genetic basis for the excellent growth performance of Boer goats but also provides new insights into the molecular regulation of muscle development.

DATA AVAILABILITY

All data in this article can be downloaded from the NCBI (PRJNA843937), GSA (PRJCA013855), and Science Data Bank databases (DOI:10.57760/sciencedb.j00139.00043).

SUPPLEMENTARY DATA

Supplementary data to this article can be found online.

COMPETING INTERESTS

The authors declare that they have no competing interests.

AUTHORS' CONTRIBUTIONS

Y.Y., W.Y.Z., and G.X.E. designed the project. B.G.Y., D.K.Z., L.X., and Y.M.H. contributed to blood sample collection. H.Y.Z. and L.C.L. analyzed the data. B.O., Y.G.H., Y.Z., K.K., M.X.C., H.Z.J., H.P.Z., and Y.W.S. contributed to data collection for experimental validation. Y.Y. and G.X. E. wrote the paper. Y.H.M., W.G.Z., H.J.G., L.J., F.P.Z., L.P.Z., R.S.N., S.Z.W., X.P.J., J.L.H., H.L., Y.F.H., Y.J.Z., and Z.Q.Z. reviewed and edited the manuscript. All authors read and approved the final version of the manuscript.

ACKNOWLEDGEMENTS

The authors thank Dr. Zhu-Qing Zheng for help in software analysis.

REFERENCES

Adewoye AB, Shrine N, Odenthal-Hesse L, et al. 2018. Human *CCL3L1* copy number variation, gene expression, and the role of the CCL3L1-CCR5 axis in lung function. *Wellcome Open Research*, **3**: 13.

Ather JL, Poynter ME. 2018. Serum amyloid A3 is required for normal weight and immunometabolic function in mice. *PLoS One*, **13**(2): e0192352.

Bassères DS, Tizzei EV, Duarte AAS, et al. 2002. ARHGAP10, a novel human gene coding for a potentially cytoskeletal Rho-GTPase activating protein. *Biochemical and Biophysical Research Communications*, **294**(3): 579−585.

Berkel C, Cacan E. 2022. Copy number and expression of CEP89, a protein

required for ciliogenesis, are increased and predict poor prognosis in patients with ovarian cancer. *Cell Biochemistry & Function*, **40**(3): 298−309.
Bezerra H, Santos E, Oliveira J, et al. 2019. Performance and ruminal parameters of boer crossbred goats fed diets that contain crude glycerin. *Animals*, **9**(11): 967.
Bi Y, He LB, Feng B, et al. 2021. A 5-bp mutation within *MSTN/GDF8* gene was significantly associated with growth traits in Inner Mongolia White Cashmere goats. *Animal Biotechnology*, **32**(5): 610−615.
Boskovic S, Marín-Juez R, Jasnic J, et al. 2018. Characterization of zebrafish (*Danio rerio*) muscle ankyrin repeat proteins reveals their conserved response to endurance exercise. *PLoS One*, **13**(9): e0204312.
Buford TW, Cooke MB, Willoughby DS. 2009. Resistance exercise-induced changes of inflammatory gene expression within human skeletal muscle. *European Journal of Applied Physiology*, **107**(4): 463−471.
Castronovo C, Crippa M, Bestetti I, et al. 2015. Complex *de novo* chromosomal rearrangement at 15q11-q13 involving an intrachromosomal triplication in a patient with a severe neuropsychological phenotype: clinical report and review of the literature. *Amercian Journal of Medical Genetics Part A*, **167**(1): 221−230.
Chang NC, Rudnicki MA. 2014. Satellite cells: the architects of skeletal muscle. *Current Topics in Developmental Biology*, **107**: 161−181.
Chaosap C, Sitthigripong R, Sivapirunthep P, et al. 2020. Myosin heavy chain isoforms expression, calpain system and quality characteristics of different muscles in goats. *Food Chemistry*, **321**: 126677.
Chinen T, Yamazaki K, Hashimoto K, et al. 2021. Centriole and PCM cooperatively recruit CEP192 to spindle poles to promote bipolar spindle assembly. *Journal of Cell Biology*, **220**(2): e202006085.
Christensen KL, Brennan JDG, Aldridge CS, et al. 2007. Cell cycle regulation of the human Six1 homeoprotein is mediated by APC^{Cdh1}. *Oncogene*, **26**(23): 3406−3414.
Cisternas P, Henriquez JP, Brandan E, et al. 2014. Wnt signaling in skeletal muscle dynamics: myogenesis, neuromuscular synapse and fibrosis. *Molecular Neurobiology*, **49**(1): 574−589.
Delaney K, Kasprzycka P, Ciemerych MA, et al. 2017. The role of TGF-β1 during skeletal muscle regeneration. *Cell Biology International*, **41**(7): 706−715.
Dodson MV, Hausman GJ, Guan LL, et al. 2010. Skeletal muscle stem cells from animals I. Basic cell biology. *International Journal of Biological Sciences*, **6**(5): 465−474.
Douglas TC, Hannila SS. 2022. Working from within: how secretory leukocyte protease inhibitor regulates the expression of pro-inflammatory genes. *Biochemistry and Cell Biology*, **100**(1): 1−8.
Dumont NA, Bentzinger CF, Sincennes MC, et al. 2015. Satellite cells and skeletal muscle regeneration. *Comprehensive Physiology*, **5**(3): 1027−1059.
Elia D, Madhala D, Ardon E, et al. 2007. Sonic hedgehog promotes proliferation and differentiation of adult muscle cells: involvement of MAPK/ERK and PI3K/Akt pathways. *Biochimica et Biophysica Acta* (*BBA*)-*Molecular Cell Research*, **1773**(9): 1438–1446.
Feng XS, Naz F, Juan AH, et al. 2018. Identification of skeletal muscle satellite cells by immunofluorescence with Pax7 and laminin antibodies. *Journal of Visualized Experiments:JoVE*, (134): 57212.
Giampietri C, Petrungaro S, Coluccia P, et al. 2010. c-Flip overexpression affects satellite cell proliferation and promotes skeletal muscle aging. *Cell Death & Disease*, **1**(4): e38.
Giordani L, Parisi A, Le Grand F. 2018. Satellite cell self-renewal. *Current Topics in Developmental Biology*, **126**: 177−203.
Howard ZM, Rastogi N, Lowe J, et al. 2022. Myeloid mineralocorticoid receptors contribute to skeletal muscle repair in muscular dystrophy and acute muscle injury. *American Journal of Physiology-Cell Physiology*, **322**(3): C354−C369.
Huang YZ, Li YJ, Wang XH, et al. 2021. An atlas of CNV maps in cattle, goat and sheep. *Science China Life Sciences*, **64**(10): 1747−1764.
Hughes JF, Coffin JM. 2001. Evidence for genomic rearrangements mediated by human endogenous retroviruses during primate evolution. *Nature Genetics*, **29**(4): 487−489.
Humayun A, Fornace AJ Jr. 2022. GADD45 in stress signaling, cell cycle control, and apoptosis. *In*: Zaidi MR, Liebermann DA. Gadd45 Stress Sensor Genes. Cham: Springer, 1–22.
Ibrahimi A, Bonen A, Blinn WD, et al. 1999. Muscle-specific overexpression of FAT/CD36 enhances fatty acid oxidation by contracting muscle, reduces plasma triglycerides and fatty acids, and increases plasma glucose and insulin. *Journal of Biological Chemistry*, **274**(38): 26761−26766.
Ji A, Trumbauer AC, Noffsinger VP, et al. 2022. Serum Amyloid A is not obligatory for high-fat, high-sucrose, cholesterol-fed diet-induced obesity and its metabolic and inflammatory complications. *PLoS One*, **17**(4): e0266688.
Kemp JR, Longworth MS. 2015. Crossing the LINE toward genomic instability: LINE-1 retrotransposition in cancer. *Frontiers in Chemistry*, **3**: 68.
Kholif AE, Hamdon HA, Kassab AY, et al. 2020. *Chlorella vulgaris* microalgae and/or copper supplementation enhanced feed intake, nutrient digestibility, ruminal fermentation, blood metabolites and lactational performance of Boer goat. *Journal of Animal Physiology and Animal Nutrition*, **104**(6): 1595−1605.
Kobayashi Y, Yoshimoto Y, Yamamoto Y, et al. 2016. Roles of EDNs in regulating oviductal NO synthesis and smooth muscle motility in cows. *Reproduction*, **151**(6): 615−622.
Kot P, Yasuhara T, Shibata A, et al. 2021. Mechanism of chromosome rearrangement arising from single-strand breaks. *Biochemical and Biophysical Research Communications*, **572**: 191−196.
Kurosaka M, Ogura Y, Funabashi T, et al. 2017. Early growth response 3 (Egr3) contributes a maintenance of C2C12 myoblast proliferation. *Journal of Cellular Physiology*, **232**(5): 1114−1122.
Ladeira GC, Pilonetto F, Fernandes AC, et al. 2022. CNV detection and their association with growth, efficiency and carcass traits in Santa Inês sheep. *Journal of Animal Breeding and Genetics*, **139**(4): 476−487.
Legoedec J, Gasque P, Jeanne JF, et al. 1995. Expression of the complement alternative pathway by human myoblasts *in vitro*: biosynthesis of C3, factor B, factor H and factor I. *European Journal of Immunology*, **25**(12): 3460−3466.
Li B, Dewey CN. 2011. RSEM: accurate transcript quantification from RNA-Seq data with or without a reference genome. *BMC Bioinformatics*, **12**: 323.
Liu M, Zhou Y, Rosen BD, et al. 2019. Diversity of copy number variation in the worldwide goat population. *Heredity*, **122**(5): 636−646.
Liu YX, Ma XM, Xiong L, et al. 2021. Effects of intensive fattening with total mixed rations on carcass characteristics, meat quality, and meat chemical composition of yak and mechanism based on serum and transcriptomic profiles. *Frontiers in Veterinary Science*, **7**: 599418.
Livak KJ, Schmittgen TD. 2001. Analysis of relative gene expression data using real-time quantitative PCR and the 2(-Delta Delta C(T)) Method. *Methods*, **25**(4): 402−408.
Love MI, Huber W, Anders S. 2014. Moderated estimation of fold change and dispersion for RNA-seq data with DESeq2. *Genome Biology*, **15**(12): 550.
Lye ZN, Purugganan MD. 2019. Copy number variation in domestication. *Trends in Plant Science*, **24**(4): 352−365.
Malan SW. 2000. The improved Boer goat. *Small Ruminant Research*, **36**(2): 165−170.
Marques JI, Leite PG, Lopes Neto JP, et al. 2021. Estimation of heat exchanges in Boer crossbred goats maintained in a climate chamber. *Journal of Thermal Biology*, **96**: 102832.
McGurk PD, Swartz ME, Chen JW, et al. 2017. *In vivo* zebrafish morphogenesis shows Cyp26b1 promotes tendon condensation and

musculoskeletal patterning in the embryonic jaw. *PLoS Genetics*, **13**(12): e1007112.

Metzger K, Tuchscherer A, Palin MF, et al. 2020. Establishment and validation of cell pools using primary muscle cells derived from satellite cells of pig skeletal muscle. *In Vitro Cellular & Developmental Biology. Animal*, **56**(3): 193−199.

Milewska M, Grabiec K, Grzelkowska-Kowalczyk K. 2014. Interactions of proliferation and differentiation signaling pathways in myogenesis. *Postepy Higieny I Medycyny Doswiadczalnej* (*Online*), **68**: 516–526.

Nasa I, Trinkle-Mulcahy L, Douglas P, et al. 2017. Recruitment of PP1 to the centrosomal scaffold protein CEP192. *Biochemical and Biophysical Research Communications*, **484**(4): 864−870.

Ncube KT, Dzomba EF, Hadebe K, et al. 2022. Carcass quality profiles and associated genomic regions of south african goat populations investigated using goat SNP50K genotypes. *Animals* (*Basel*), **12**(3): 364.

Ogura Y, Sato S, Kurosaka M, et al. 2020. Age-related decrease in muscle satellite cells is accompanied with diminished expression of early growth response 3 in mice. *Molecular Biology Reports*, **47**(2): 977−986.

Okano J, Sakai Y, Shiota K. 2008. Retinoic acid down-regulates *Tbx1* expression and induces abnormal differentiation of tongue muscles in fetal mice. *Developmental Dynamics*, **237**(10): 3059−3070.

Paudel Y, Madsen O, Megens HJ, et al. 2013. Evolutionary dynamics of copy number variation in pig genomes in the context of adaptation and domestication. *BMC Genomics*, **14**: 449.

Pérez-Baena I, Jarque-Durán M, Gómez EA, et al. 2021. Terminal crossbreeding of murciano-granadina goats to boer bucks: effects on reproductive performance of goats and growth of kids in artificial rearing. *Animals* (*Basel*), **11**(4): 986.

Pielberg G, Day AE, Plastow GS, et al. 2003. A sensitive method for detecting variation in copy numbers of duplicated genes. *Genome Research*, **13**(9): 2171−2177.

Poleti MD, DeRijk RH, Rosa AF, et al. 2015. Genetic variants in glucocorticoid and mineralocorticoid receptors are associated with concentrations of plasma cortisol, muscle glycogen content, and meat quality traits in male Nellore cattle. *Domestic Animal Endocrinology*, **51**: 105−113.

Relaix F, Zammit PS. 2012. Satellite cells are essential for skeletal muscle regeneration: the cell on the edge returns centre stage. *Development*, **139**(16): 2845−2856.

Rudolf A, Schirwis E, Giordani L, et al. 2016. β-Catenin activation in muscle progenitor cells regulates tissue repair. *Cell Reports*, **15**(6): 1277−1290.

Sato T, Kawamura Y, Asai R, et al. 2008. Recombinase-mediated cassette exchange reveals the selective use of G_q/G_{11}-dependent and -independent endothelin 1/endothelin type A receptor signaling in pharyngeal arch development. *Development*, **135**(4): 755−765.

Scheja L, Heese B, Zitzer H, et al. 2008. Acute-phase serum amyloid A as a marker of insulin resistance in mice. *Journal of Diabetes Research*, **2008**: 230837.

Schulze-Topphoff U, Prat A, Prozorovski T, et al. 2009. Activation of kinin receptor B1 limits encephalitogenic T lymphocyte recruitment to the central nervous system. *Nature Medicine*, **15**(7): 788−793.

Shakweer WMES, El-Rahman HHA. 2020. Cloning, nucleotide sequencing, and bioinformatics analyses of growth hormone mRNA of Assaf sheep and Boer goats reared in Egypt. *Journal of Genetic Engineering and Biotechnology*, **18**(1): 30.

Shao X, Lv N, Liao J, et al. 2019. Copy number variation is highly correlated with differential gene expression: a pan-cancer study. *BMC Medical Genetics*, **20**(1): 175.

Shen Y, Yan YL, Liu YQ, et al. 2013. A significant effect of the *TSPY1* copy number on spermatogenesis efficiency and the phenotypic expression of the gr/gr deletion. *Human Molecular Genetics*, **22**(8): 1679−1695.

Shibata H, Oishi K, Yamagiwa A, et al. 2001. PKNβ interacts with the SH3 domains of Graf and a novel Graf related protein, Graf 2, which are GTPase activating proteins for Rho family. *The Journal of Cellular Biochemistry*, **130**(1): 23−31.

Shishido E, Aleksic B, Ozaki N. 2014. Copy-number variation in the pathogenesis of autism spectrum disorder. *Psychiatry and Clinical Neurosciences*, **68**(2): 85−95.

Su XT, Zhao YF, Wang YN, et al. 2018. Overexpression of the *Rybp* gene inhibits differentiation of bovine myoblasts into myotubes. *International Journal of Molecular Sciences*, **19**(7): 2082.

Sun DP, Lee YW, Chen JT, et al. 2020. The bradykinin-BDKRB1 axis regulates *Aquaporin 4* gene expression and consequential migration and invasion of malignant glioblastoma cells via a Ca^{2+}-MEK1-ERK1/2-NF-κB mechanism. *Cancers* (*Basel*), **12**(3): 667.

Tsai AG, Lieber MR. 2010. Mechanisms of chromosomal rearrangement in the human genome. *BMC Genomics*, **11 Suppl 1**(Suppl 1): S1.

Ueda S, Hosoda M, Yoshino KI, et al. 2021. Gene expression analysis provides new insights into the mechanism of intramuscular fat formation in japanese black cattle. *Genes* (*Basel*), **12**(8): 1107.

Uhlar CM, Whitehead AS. 1999. Serum amyloid A, the major vertebrate acute-phase reactant. *European Journal of Biochemistry*, **265**(2): 501−523.

van Wyk GL, Hoffman LC, Strydom PE, et al. 2022. Differences in meat quality of six muscles obtained from southern african large-frame indigenous veld goat and boer goat wethers and bucks. *Animals* (*Basel*), **12**(3): 382.

Veal CD, Reekie KE, Lorentzen JC, et al. 2014. A 129-kb deletion on chromosome 12 confers substantial protection against rheumatoid arthritis, implicating the gene *SLC2A3*. *Human Mutation*, **35**(2): 248–256.

Verpoorten S, Sfyri P, Scully D, et al. 2020. Loss of CD36 protects against diet-induced obesity but results in impaired muscle stem cell function, delayed muscle regeneration and hepatic steatosis. *Acta Physiologica*, **228**(3): e13395.

Wan FQ, Ma FL, Wu JX, et al. 2022. Effect of *Lycium barbarum* polysaccharide on decreasing serum amyloid A3 expression through inhibiting NF-κB activation in a mouse model of diabetic nephropathy. *Analytical Cellular Pathology*, **2022**: 7847135.

Wang J, Wang S, Luan Y, et al. 2017a. Overexpression of NEDD9 in renal cell carcinoma is associated with tumor migration and invasion. *Oncology Letters*, **14**(6): 8021−8027.

Wang LJ, Zhu YH, Liu X, et al. 2019a. Glycogen synthase kinase 3β (GSK3β) regulates the expression of MyHC2a in goat skeletal muscle satellite cells (SMSCs). *Animal Science Journal*, **90**(8): 1042−1049.

Wang WT, Sun B, Hu P, et al. 2019b. Comparison of differential flavor metabolites in meat of lubei white goat, Jining gray goat and boer goat. *Metabolites*, **9**(9): 176.

Wang XH, Zheng ZQ, Cai YD, et al. 2017b. CNVcaller: highly efficient and widely applicable software for detecting copy number variations in large populations. *Gigascience*, **6**(12): 1−12.

Wang Y, Xiao X, Wang LJ. 2020. *In vitro* characterization of goat skeletal muscle satellite cells. *Animal Biotechnology*, **31**(2): 115−121.

Wu HQ, Ren Y, Pan W, et al. 2015. The mammalian target of rapamycin signaling pathway regulates myocyte enhancer factor-2C phosphorylation levels through integrin-linked kinase in goat skeletal muscle satellite cells. *Cell Biology International*, **39**(11): 1264−1273.

Xie C, Tammi MT. 2009. CNV-seq, a new method to detect copy number variation using high-throughput sequencing. *BMC Bioinformatics*, **10**: 80.

Xiong Q, Tao H, Zhang N, et al. 2020. Skin transcriptome profiles associated with black- and white-coated regions in Boer and Macheng black crossbred goats. *Genomics*, **112**(2): 1853−1860.

Xu ZJ, Wang XW, Zhang ZJ, et al. 2020. Copy number variation of *CADM2* gene revealed its association with growth traits across Chinese *Capra*

hircus (goat) populations. *Gene*, **741**: 144519.

Yang BG, Yuan Y, Zhou DK, et al. 2021. Genome-wide selection signal analysis of Australian Boer goat reveals artificial selection imprinting on candidate genes related to muscle development. *Animal Genetics*, **52**(4): 550−555.

Yin H, Price F, Rudnicki MA. 2013. Satellite cells and the muscle stem cell niche. *Physiological Reviews*, **93**(1): 23−67.

Yin HD, Zhao J, He HR, et al. 2020. Gga-miR-3525 targets *PDLIM3* through the MAPK signaling pathway to regulate the proliferation and differentiation of skeletal muscle satellite cells. *International Journal of Molecular Sciences*, **21**(15): 5573.

Zhang PP, Liang XR, Shan TZ, et al. 2015. mTOR is necessary for proper satellite cell activity and skeletal muscle regeneration. *Biochemical and Biophysical Research Communications*, **463**(1–2): 102–108.

Zhang WY, Zhang SX, Xu YY, et al. 2019. The DNA methylation status of wnt and Tgfβ signals is a key factor on functional regulation of skeletal muscle satellite cell development. *Frontiers in Genetics*, **10**: 220.

Zhang X, Liu L, Chen C, et al. 2013. Interferon regulatory factor-1 together with reactive oxygen species promotes the acceleration of cell cycle progression by up-regulating the cyclin E and CDK2 genes during high glucose-induced proliferation of vascular smooth muscle cells. *Cardiovascular Diabetology*, **12**: 147.

Zhou HH, Chen X, Cai LY, et al. 2019. Erastin reverses ABCB1-mediated docetaxel resistance in ovarian cancer. *Frontiers in Oncology*, **9**: 1398.

Ziegler GC, Almos P, McNeill RV, et al. 2020. Cellular effects and clinical implications of *SLC2A3* copy number variation. *Journal of Cellular Physiology*, **235**(12): 9021−9036.

ZR | Zoological Research

Supplementary Materials

A 1.1 Mb duplication CNV on chromosome 17 contributes to skeletal muscle development in Boer goats

Ying Yuan[1,2,#], Wei-Yi Zhang[1,2,#], Bai-Gao Yang[1,2], Dong-Ke Zhou[1,2], Lu Xu[1,2], Yong-Meng He[1,2], Hao-Yuan Zhang[1,2], Cheng-Li Liu[1,2], Yue-Hui Ma[3], Ming-Xing Chu[3], Wen-Guang Zhang[4], Hui-Jiang Gao[3], Lin Jiang[3], Fu-Ping Zhao[3], Lu-Pei Zhang[3], Ri-Su Na[4], Baatarchogt Oyungerel[5], Yan-Guo Han[1,2], Yan Zeng[1,2], Shi-Zhi Wang[1,2], Huai-Zhi Jiang[6], Hong-Ping Zhang[7], Xun-Ping Jiang[8], Jian-Ning He[9], Hao Liang[10], Kaushalendra Kaushalendra[11], Ya-Wang Sun[1,2], Yong-Fu Huang[1,2], Yong-Ju Zhao[1,2], Zhong-Quan Zhao[1,2], Guang-Xin E[1,2,*]

1. College of Animal Science and Technology, Southwest University, Chongqing 400715, China
2. Chongqing Key Laboratory of Forage & Herbivore, Chongqing 400715, China
3. Institute of Animal Science, Chinese Academy of Agricultural Sciences (CAAS), Beijing 100193, China
4. College of Animal Science, Inner Mongolia Agricultural University, Huhhot, Inner Mongolia 010018, China
5. School of Animal Science & Biotechnology, Mongolian University of Life Sciences, Zaisan, Khan-uul, Ulaanbaatar 17024, Mongolia
6. Animal Science and Technology College, Jilin Agriculture University, Changchun, Jilin 130118, China
7. Farm Animal Genetic Resources Exploration and Innovation Key Laboratory of Sichuan Province, College of Animal Science and Technology, Sichuan Agricultural University, Chengdu, Sichuan 611130, China
8. Key Lab of Agricultural Animal, Genetics, Breeding and Reproduction of Ministry of Education, College of Animal Science and Technology, Huazhong, Agricultural University, Wuhan, Hubei 430070, China
9. College of Animal Science and Technology, Qingdao Agricultural University, Qingdao, Shandong 266109, China
10. State Key Laboratory of Reproductive Regulation and Breeding of Grassland Livestock, School of Life Sciences, Inner Mongolia University, Hohhot, Inner Mongolia 010070, China
11. Department of Zoology, Pachhunga University College, Mizoram University, Aizawl 796001, India

[#]Authors contributed equally to this work
[*]Corresponding author, E-mail: eguangxin@126.com

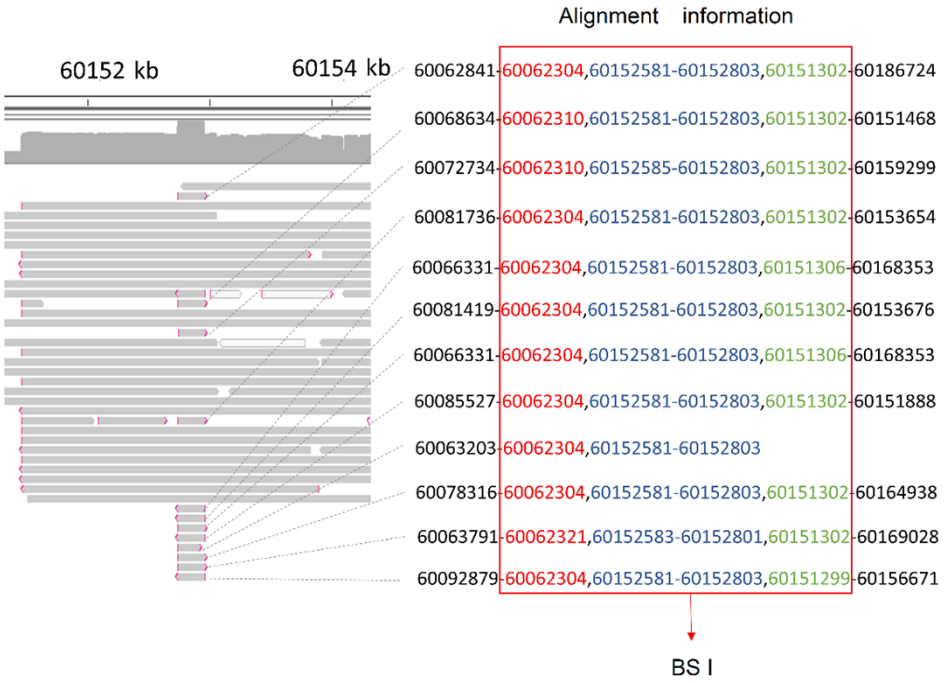

Supplementary Figure S1 Multicopy element 1 (MCE1) alignment information based on IGV

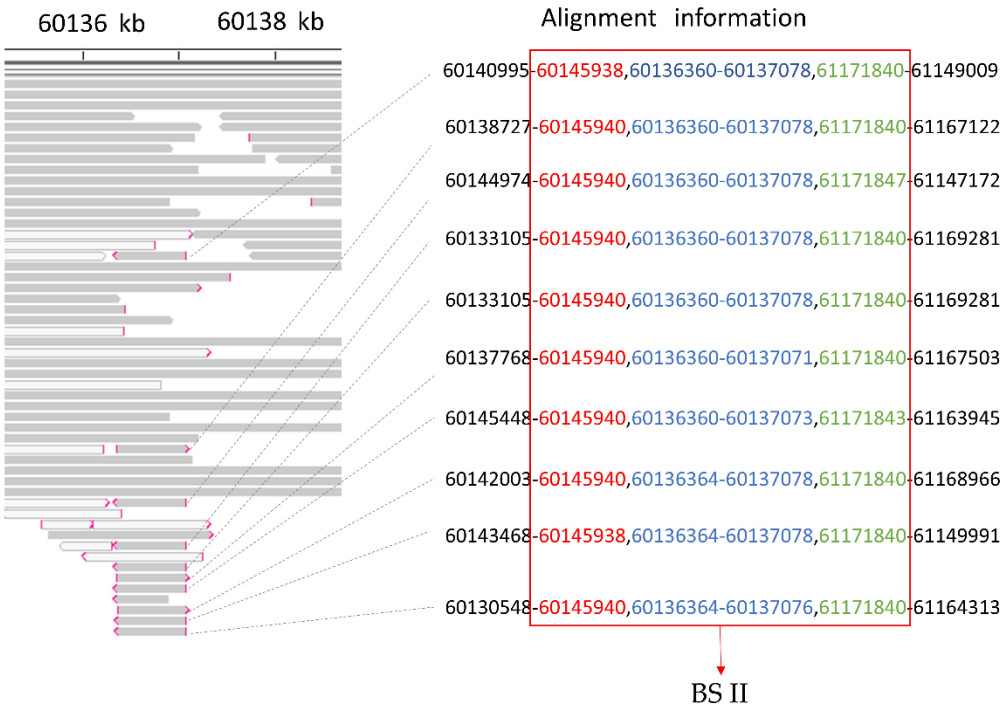

Supplementary Figure S2 Multicopy element 2 (MCE2) alignment information based on IGV

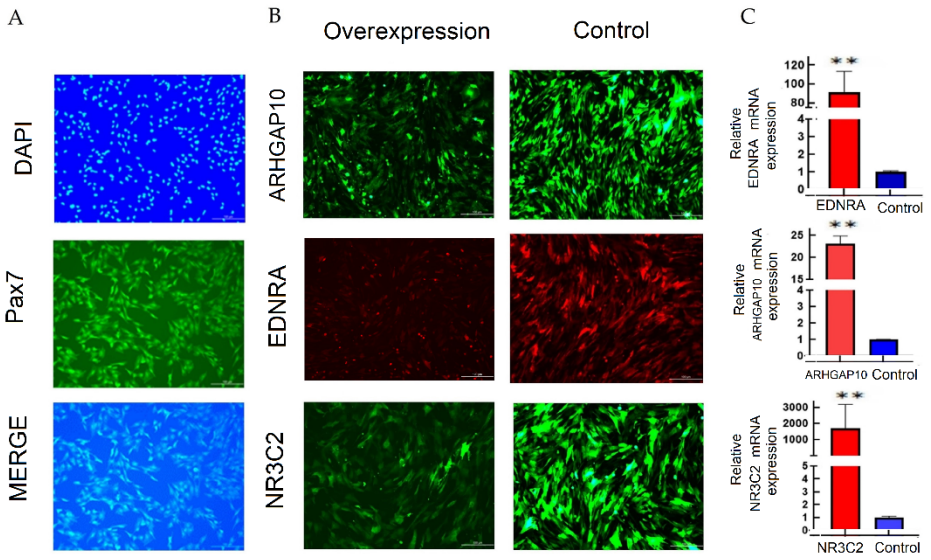

Supplementary Figure S3 Culture, identification, and lentiviral transfection of SMSCs (A). Immunofluorescence of Pax7 in SMSCs of Dazu black goat at 7 days. (B). Fluorescence effects of SMSCs in goats after overexpression and transfection of *ARHGAP10*, *NR3C2*, and *EDNRA*. (C). mRNA expression of *ARHGAP10*, *NR3C2* and *EDNRA* in SMSCs following transfection with overexpressed candidate genes. Data are mean±SEM (n=6). * P<0.05; ** P<0.01 vs. Control.

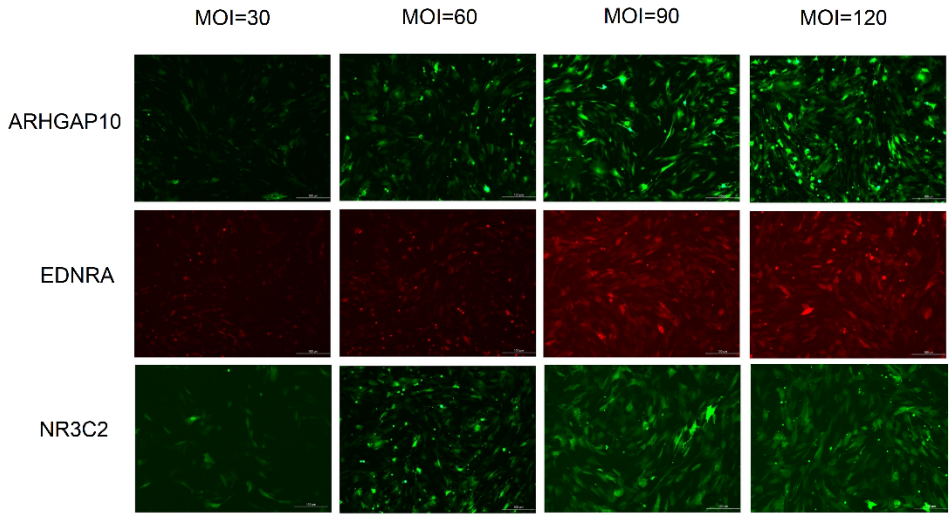

Supplementary Figure S4 Infection efficiencies at different multiplicities of infection (MOI: 30, 60, 90, and 120)

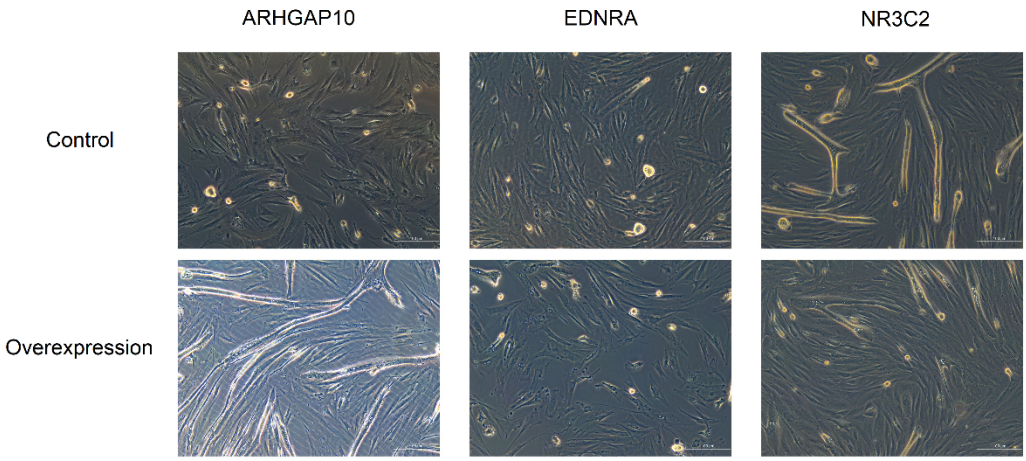

Supplementary Figure S5 Effects of SMSCs differentiation after 4 days

Supplementary Table S1 Basic information and data read-depth of 127 individuals for genome-wide selection signal analysis

Group	SRA Accesion	Gender	Reads_depth	Type	Region	Description	Data Source
Case	SAMN16533891	F	12.609X	Domestic	Australia	Boer Goat	Our previous published project
Case	SAMN16533892	F	13.3679X	Domestic	Australia	Boer Goat	Our previous published project
Case	SAMN16533893	F	14.3808X	Domestic	Australia	Boer Goat	Our previous published project
Case	SAMN16533894	F	11.7929X	Domestic	Australia	Boer Goat	Our previous published project
Case	SAMN16533895	F	13.5393X	Domestic	Australia	Boer Goat	Our previous published project
Case	SAMN16533896	F	12.4078X	Domestic	Australia	Boer Goat	Our previous published project
Case	SAMN16533897	F	11.0125X	Domestic	Australia	Boer Goat	Our previous published project
Case	SAMN16533898	F	10.8238X	Domestic	Australia	Boer Goat	Our previous published project
Case	SAMN16533899	F	12.8495X	Domestic	Australia	Boer Goat	Our previous published project
Case	SAMN16533900	F	11.9781X	Domestic	Australia	Boer Goat	Our previous published project
Case	SAMN16533901	F	11.5509X	Domestic	Australia	Boer Goat	Our previous published project
Case	SAMN16533902	F	11.5959X	Domestic	Australia	Boer Goat	Our previous published project
Case	SAMN16533903	F	11.0733X	Domestic	Australia	Boer Goat	Our previous published project
Case	SAMN16533904	F	11.8124X	Domestic	Australia	Boer Goat	Our previous published project
Case	SAMN16533905	F	106348X	Domestic	Australia	Boer Goat	Our previous published project
Case	SAMN16533906	F	11.3519X	Domestic	Australia	Boer Goat	Our previous published project
Case	SAMN16533907	F	12.085X	Domestic	Australia	Boer Goat	Our previous published project
Case	SAMN16533908	F	11.5349X	Domestic	Australia	Boer Goat	Our previous published project
Case	SAMN16533909	F	11.634X	Domestic	Australia	Boer Goat	Our previous published project
Case	SAMN16533910	F	12.9826X	Domestic	Australia	Boer Goat	Our previous published project
Case	SAMN16533911	F	10.3204X	Domestic	Australia	Boer Goat	Our previous published project
Case	SAMN16533912	F	13.0995X	Domestic	Australia	Boer Goat	Our previous published project
Case	SAMN16533913	F	11.7212X	Domestic	Australia	Boer Goat	Our previous published project
Case	SAMN16533914	F	13.8885X	Domestic	Australia	Boer Goat	Our previous published project
Case	SAMN16533915	F	11.2494X	Domestic	Australia	Boer Goat	Our previous published project
Case	SAMN16533916	F	13.344X	Domestic	Australia	Boer Goat	Our previous published project
Case	SAMN16533917	F	14.5771X	Domestic	Australia	Boer Goat	Our previous published project
Case	SAMN16533918	F	13.6178X	Domestic	Australia	Boer Goat	Our previous published project
Case	SAMN16533919	F	12.6628X	Domestic	Australia	Boer Goat	Our previous published project
Case	SAMN16533920	F	11.6456X	Domestic	Australia	Boer Goat	Our previous published project
Case	SAMN16533921	F	10.247X	Domestic	Australia	Boer Goat	Our previous published project
Case	SAMN16533922	F	10.3176X	Domestic	Australia	Boer Goat	Our previous published project
Case	SAMN16533923	F	11.7862X	Domestic	Australia	Boer Goat	Our previous published project
Case	SAMN16533924	F	12.8952X	Domestic	Australia	Boer Goat	Our previous published project
Case	SAMN16533925	F	14.3407X	Domestic	Australia	Boer Goat	Our previous published project
Case	SAMN16533926	F	13.122X	Domestic	Australia	Boer Goat	Our previous published project
Case	SAMN16533927	F	15.2178X	Domestic	Australia	Boer Goat	Our previous published project
Case	SAMN16533928	F	11.837X	Domestic	Australia	Boer Goat	Our previous published project
Case	SAMN16533929	F	11.778X	Domestic	Australia	Boer Goat	Our previous published project
Case	SAMN16533930	F	11.7308X	Domestic	Australia	Boer Goat	Our previous published project
Case	SAMN16533931	F	12.5788X	Domestic	Australia	Boer Goat	Our previous published project

Case	SAMN16533932	F	10.7098X	Domestic	Australia	Boer Goat	Our previous published project
Case	SAMN16533933	F	11.0337X	Domestic	Australia	Boer Goat	Our previous published project
Case	SAMN16533934	F	11.0633X	Domestic	Australia	Boer Goat	Our previous published project
Case	SAMN16533935	F	11.4193X	Domestic	Australia	Boer Goat	Our previous published project
Case	SAMN16533936	F	10.8282X	Domestic	Australia	Boer Goat	Our previous published project
Control	SRR5803210	F	8.2348X	Domestic	Africa	Red_Sokoto_Nigeria_Africa	Download
Control	SRR5803208	F	10.8372X	Domestic	Africa	West_African_Dwarf_West_Africa_	Download
Control	SRR5803191	F	11.0302X	Domestic	Africa	Borena_goat_Ethiopia	Download
Control	ERR219543	M	12.6745X	Domestic	Africa	Moukrissat	Download
Control	ERR219546	M	13.4799X	Domestic	Africa	Kerrandou	Download
Control	ERR229471	M	13.2196X	Domestic	Africa	ait_Hani	Download
Control	ERR229474	M	12.7225X	Domestic	Africa	Mssissi	Download
Control	ERR229476	M	13.354X	Domestic	Africa	Skoura	Download
Control	ERR229478	F	13.5109X	Domestic	Africa	Taglefte	Download
Control	ERR229479	F	12.0271X	Domestic	Africa	Tabante	Download
Control	ERR229481	M	13.4953X	Domestic	Africa	Tabante	Download
Control	ERR229484	F	15.0498X	Domestic	Africa	Beni_Smir	Download
Control	ERR229485	M	12.8365X	Domestic	Africa	Chorafa_M'daghr	Download
Control	ERR229487	M	13.1419X	Domestic	Africa	Tabante	Download
Control	ERR232492	M	12.262X	Domestic	Africa	Tabouchit	Download
Control	ERR234304	F	12.1474X	Domestic	Africa	Tizagtaouine	Download
Control	ERR234305	F	13.4394X	Domestic	Africa	Adis	Download
Control	ERR234315	M	13.5459X	Domestic	Africa	TAGHJIJT	Download
Control	ERR246143	F	12.1994X	Domestic	Africa	Taliouine	Download
Control	ERR246152	M	13.762X	Domestic	Africa	Al_hajeb	Download
Control	ERR246153	F	14.6321X	Domestic	Africa	Tiisent	Download
Control	ERR248926	F	13.4682X	Domestic	Africa	Zhiliga	Download
Control	ERR248928	F	14.5546X	Domestic	Africa	Kelaat_Megouna	Download
Control	ERR248929	F	13.6323X	Domestic	Africa	TANTAN	Download
Control	ERR248933	F	13.4938X	Domestic	Africa	Agoudi_El_Khair	Download
Control	ERR299283	M	13.6174X	Domestic	Africa	unknown	Download
Control	ERR313257	M	12.2335X	Domestic	Africa	Taouloukoult	Download
Control	ERR313258	M	13.2107X	Domestic	Africa	Mzizel	Download
Control	ERR313259	M	15.0561X	Domestic	Africa	Amrsid	Download
Control	ERR313266	M	12.3525X	Domestic	Africa	Zaouyat_Bellemkaddem	Download

Control	ERR313272	M	13.4437X	Domestic	Africa	Smimou	Download
Control	ERR315500	M	13.2539X	Domestic	Africa	ABAYNO	Download
Control	ERR315503	F	15.7587X	Domestic	Africa	Adis	Download
Control	ERR315505	M	13.4852X	Domestic	Africa	ASRIR	Download
Control	ERR315508	F	14.2071X	Domestic	Africa	TAGHJIJT	Download
Control	ERR315510	F	12.665X	Domestic	Africa	Oum_Gerdan	Download
Control	ERR315512	F	12.3768X	Domestic	Africa	Tarmigte	Download
Control	ERR315515	M	11.8881X	Domestic	Africa	Ousalsat	Download
Control	ERR315516	M	14.4249X	Domestic	Africa	Akka	Download
Control	ERR315795	M	11.9326X	Domestic	Africa	Rmila	Download
Control	ERR318768	M	12.8828X	Domestic	Africa	Ayir	Download
Control	ERR332592	M	11.8571X	Domestic	Africa	Tetouan	Download
Control	ERR340428	M	12.8949X	Domestic	Africa	Asjen	Download
Control	ERR345973	M	11.5333X	Domestic	Africa	Moulay_bouazza	Download
Control	SRR5803188	F	9.7426X	Domestic	Africa	Short_eared_Somali_Ethiopia	Download
Control	SRR5803235	M	13.8259X	Domestic	Europe	France_Alpine	Download
Control	SRR5803234	M	13.5604X	Domestic	Europe	Dries_Netherlands	Download
Control	SRR5803227	F	14.0092X	Domestic	Europe	Terry_Netherlands	Download
Control	ERR405774	F	14.1132X	Domestic	Europe		Download
Control	ERR405775	F	14.4178X	Domestic	Europe		Download
Control	ERR405776	F	13.6873X	Domestic	Europe		Download
Control	ERR405777	F	13.8459X	Domestic	Europe		Download
Control	ERR405778	F	13.6748X	Domestic	Europe		Download
Control	ERR470101	F	13.4456X	Domestic	Europe	Saanen	Download
Control	ERR470102	F	13.245X	Domestic	Europe	Saanen	Download
Control	ERR470103	F	14.2284X	Domestic	Europe	Alpine	Download
Control	ERR470105	F	13.8856X	Domestic	Europe	Alpine	Download
Control	SRR5803174	M	14.3994X	Domestic	Europe	Poitou_goat_Western_France	Download
Control	SRR5803226	M	11.1063X	Domestic	Europe	Saanen_Netherlands	Download
Control	SRR5803232	F	13.8015X	Domestic	Europe	Spain_goat_Spain	Download
Control	SRR5803173	F	10.4407X	Domestic	Europe	Spain_goat_Spain	Download
Control	SRR10613891	F	9.2587X	Domestic	Asia	Tangshan_milk_goat	Our previous published project

Control	SRR10613890	F	8.7454X	Domestic	Asia	Tangshan_milk_goat	Our previous published project
Control	SRR10613879	F	10.8614X	Domestic	Asia	Tangshan_milk_goat	Our previous published project
Control	SRR10613878	F	11.4991X	Domestic	Asia	Tangshan_milk_goat	Our previous published project
Control	SRR10613877	F	9.1489X	Domestic	Asia	Tangshan_milk_goat	Our previous published project
Control	SRR10613876	F	9.138X	Domestic	Asia	Tangshan_milk_goat	Our previous published project
Control	SRR10613875	F	9.1288X	Domestic	Asia	Tangshan_milk_goat	Our previous published project
Control	SRR10613874	F	9.3693X	Domestic	Asia	Tangshan_milk_goat	Our previous published project
Control	SRR10613873	F	9.2895X	Domestic	Asia	Tangshan_milk_goat	Our previous published project
Control	SRR10613872	F	9.1213X	Domestic	Asia	Tangshan_milk_goat	Our previous published project
Control	SRR10613889	F	9.4301X	Domestic	Asia	Tangshan_milk_goat	Our previous published project
Control	SRR10613888	F	9.2358X	Domestic	Asia	Tangshan_milk_goat	Our previous published project
Control	SRR10613887	F	9.1578X	Domestic	Asia	Tangshan_milk_goat	Our previous published project
Control	SRR10613886	F	9.4332X	Domestic	Asia	Tangshan_milk_goat	Our previous published project
Control	SRR10613885	F	9.3515X	Domestic	Asia	Tangshan_milk_goat	Our previous published project
Control	SRR10613884	F	9.3073X	Domestic	Asia	Tangshan_milk_goat	Our previous published project
Control	SRR10613883	F	9.4888X	Domestic	Asia	Tangshan_milk_goat	Our previous published project
Control	SRR10613882	F	9.0719X	Domestic	Asia	Tangshan_milk_goat	Our previous published project
Control	SRR10613881	F	9.5443X	Domestic	Asia	Tangshan_milk_goat	Our previous published project
Control	SRR10613880	F	9.2899X	Domestic	Asia	Tangshan_milk_goat	Our previous published project

Supplementary Table S2 Basic information and data read-depth of 80 Chinese goats

Gender	Reads_depth	Type	Region	Description	SRA Accesion
F	10X	Domestic	Chongqing,China,Asia	Dazu Black Goat	SAMN19316008
F	10X	Domestic	Chongqing,China,Asia	Dazu Black Goat	SAMN19316011
F	10X	Domestic	Chongqing,China,Asia	Dazu Black Goat	SAMN19316007
F	10X	Domestic	Chongqing,China,Asia	Dazu Black Goat	SAMN19316001
F	10X	Domestic	Chongqing,China,Asia	Dazu Black Goat	SAMN19315993
F	10X	Domestic	Chongqing,China,Asia	Dazu Black Goat	SAMN19316002
F	10X	Domestic	Chongqing,China,Asia	Dazu Black Goat	SAMN19316000
F	10X	Domestic	Chongqing,China,Asia	Dazu Black Goat	SAMN19316005
F	10X	Domestic	Chongqing,China,Asia	Dazu Black Goat	SAMN19315992
F	10X	Domestic	Chongqing,China,Asia	Dazu Black Goat	SAMN19316003
F	10X	Domestic	Chongqing,China,Asia	Dazu Black Goat	SAMN19315996
F	10X	Domestic	Chongqing,China,Asia	Dazu Black Goat	SAMN19316004
F	10X	Domestic	Chongqing,China,Asia	Dazu Black Goat	SAMN19315994
F	10X	Domestic	Chongqing,China,Asia	Dazu Black Goat	SAMN19315995
F	10X	Domestic	Chongqing,China,Asia	Dazu Black Goat	SAMN19315997
F	10X	Domestic	Chongqing,China,Asia	Dazu Black Goat	SAMN19315998
F	10X	Domestic	Chongqing,China,Asia	Dazu Black Goat	SAMN19316006
F	10X	Domestic	Chongqing,China,Asia	Dazu Black Goat	SAMN19315999
F	10X	Domestic	Chongqing,China,Asia	Dazu Black Goat	SAMN19523150
F	10X	Domestic	Chongqing,China,Asia	Dazu Black Goat	SAMN19316014
F	10X	Domestic	Chongqing,China,Asia	Dazu Black Goat	SAMN19316013
F	10X	Domestic	Chongqing,China,Asia	Dazu Black Goat	SAMN19316009
F	10X	Domestic	Chongqing,China,Asia	Dazu Black Goat	SAMN19316010
F	10X	Domestic	Chongqing,China,Asia	Hechuan White Goat	SAMN19523158
F	10X	Domestic	Chongqing,China,Asia	Hechuan White Goat	SAMN19523159
F	10X	Domestic	Chongqing,China,Asia	Hechuan White Goat	SAMN19523161
F	10X	Domestic	Chongqing,China,Asia	Hechuan White Goat	SAMN19523162
F	10X	Domestic	Chongqing,China,Asia	Hechuan White Goat	SAMN19523151
F	10X	Domestic	Chongqing,China,Asia	Hechuan White Goat	SAMN19523156
F	10X	Domestic	Chongqing,China,Asia	Hechuan White Goat	SAMN19523154
F	10X	Domestic	Chongqing,China,Asia	Hechuan White Goat	SAMN19523160
F	10X	Domestic	Chongqing,China,Asia	Hechuan White Goat	SAMN19523155
F	10X	Domestic	Chongqing,China,Asia	Hechuan White Goat	SAMN19523166
F	10X	Domestic	Chongqing,China,Asia	Hechuan White Goat	SAMN19523157
F	10X	Domestic	Chongqing,China,Asia	Hechuan White Goat	SAMN19523164
F	10X	Domestic	Chongqing,China,Asia	Hechuan White Goat	SAMN19523163
F	10X	Domestic	Chongqing,China,Asia	Hechuan White Goat	SAMN19523152
F	10X	Domestic	Chongqing,China,Asia	Hechuan White Goat	SAMN19523165

Supplementary Table S3 Information on PCR amplification primers for HSV

	Forward primer 5'→3'	Reverse primer 5'→3'
indel	AAGCATGCCAGCAAAGGTCA	TGGACAGCCTTGAGTGTGGA
BS I	TGGTGGCACTCTTCACTCAG	CATTTTGCCTTCCAACGATT
BS II	GAAGGGAGGGTGAATTGGGA	CCTTACCCGGTTTCCTCAGT

Supplementary Table S4 Information on primers for overexpressed differential gene Cdna

Target gene	Forward primer 5'→3'	Reverse primer 5'→3'
EDNRA	AGAGGATCTATTTCCGGTGAATTC	TCACTTAAGCTTGGTACCGAGGATC
	GCCACCATGGAAACTTTTTGCTCA	CTTAATGGTGATGGTGATGATGGT
ARHGAP10	TACTAGAGGATCTATTTCCGGTGAATT	TCACTTAAGCTTGGTACCGAGGAT
	CGCCACCATGGGGCTGCAG CCCCT	CCCAGCAGCTTGACGTAATTCTGT
NR3C2	ACTAGAGGATCTATTTCCGGTGAA	CACTTAAGCTTGGTACCGAGGATC
	TTCGCCACCATGGAGACCAAAGGCT	CCTTCCTGTGAAAGTAAAGGGTCTT

Supplementary Table S5 Primer information for gene qRT-PCR analysis

Gene symbol	Forward primer 5'→3'	Reverse primer 5'→3'
C2	CCACCAATCCCATCCAGCAGAAG	CCAGGAGCAGGTAGAGGTTCAGG
CYP26B1	AGGAGCACGGGAAGGAGATGAC	AGTGGTGGCATAGGCAGCAAAG
SLC7A8	CATTGAGTTGCTGACCCTGGTGAG	GCTGCTCCATGTTCTGGTTCCTATC
SLPI	ACACTTGCGGAACCGAATGTCTG	CTATGCACTGGTCGTCTGTCTCAC
CFB	GAATGGTCGGTGGGATGGAGAAAC	GACACGATCTTCAAGGCGGTACTG
EDNRA	TTGCCTCTGCTGCTGCTGTTAC	TGTCCTTGTGGCTGCTCCTCTC
XIRP2	CGGCGAACACAAACCTCTCCTAAG	GAACGACTCTTGGGTGGCGAAG
TGFB2	AGCGGAGCGACGAGGAATACTAC	CACTGAGCCAGAGGGTGTTGTAAC
SORBS2	TCCTTCCAAGACGACACCAACAAC	GTGCGGTCCTTCCAAGATCAGTC
SMARCD3	GCAGTGCCAAGAGGAGGAAGATG	AACGCCAAGAGGTCCATGTAAGC
SLC8A1	TTAGATGGAGCCCTGGTTCTGGAG	CCTTCTCTGGATGCTTCTGCTTGAG
SCN7A	TCTGCCTCTGACGGTAGGAGATTAC	GGAGGGACAGCATCAAAGGAAGC
RGS2	AAAGTGCTATGTTCCTGGCTGTCC	CTTCTCTCGCTTCTCCTCGTTCTTG
PLCB4	TGGTGATGAACAACGGTCTCAATCC	CATACACGGCGATCCTCAAGACAG
PDLIM3	AACCTAGTCAGCCTCGCCAGTC	TTCCAGCAGGACGGTCATCAGG
OGN	TGAAATGCCCACATGCCTGCTATG	GCAAAGGTGGTACAGCATCAATGTC
NR4A3	CAGAAGTGTCTCAGTGTCGGAATGG	CAGATCGGAGGAGAAGGTGGAGAG
NPPC	GCGCAAATACAAAGGAGGCAACAAG	CTAACAACCCAGGCCGCTCATG
MYORG	TCGTAAGACTCCTGAGACCGTCAC	GCTTGGGCTTGGTAGGGGAAAAG
MYLK	GTGTGCGTGCAATCAATGTCTATGG	CACTTCGTCCTTCGGCTCTTCTTC
MYH3	GCTGGCTGGAGAAGAACAAGGAC	TGGTGAAGGTGGCGTAGAGGTG
LIF	GTGAGCCATGTGGATGTGACCTAC	ACGGCAATGACCTGCTTGTACTTC
KCNJ8	CGAGGAGGAAGGTGTGTATTCTGTG	TTCTGGAGGGTCTGGATAAGGATGG
ITGA8	GGGACGACTAGGAGGAGGAGAAAG	AACTTCAAAGGACACCAGGGATGC

ITGA2	GCAACATCGCAGACATACCAACATG	GTCCACCAGCAGCCATTGAGTAAG
HAS2	TCCTACTTCCGAGAGTGGCTGTAC	AGAGCTGGATTACTGTGGCAATGAG
EGR3	TCTCTACTCGGAGCCTGTGTCTTTC	AGTCGGGAATCATGGGGAAGAGG
DSP	GCTCGGAGATGTTCGGAGATGATG	GTCGTGGTTACTGTCTGGTGCTG
CFLAR	GACACCTTCACTTTCCTGGGCTATG	CTGGGCAACCTGGCGTAGAATG
CASQ2	ACTGGATTGAGGATGTGCTTTCTGG	TGTCATCGTCATTGTCGTCGTCTTC
BMP2	GGGTGGAATGACTGGATCGTTGC	TGGACAATGGCATGATTCGTGGAG
BDKRB1	AGGTGCTGCGTAACAACGAGATG	AGGAAGGTGCTGATCTGGAAGGG
ANKRD1	AGACTCCGATGGATCTGGTGCTAC	TGTTGCTATGCGAGAGGCTTTGTAG
ADRA1B	CATCGTGGGCAACATCCTAGTCATC	CTTAGCAGCAGGTCGGCAATGG
ADCY7	CGGCATCAATCGGCACTCCTTC	CCCAATCACTCCAGCAATCACAGG
NR3C2	GCTATGACGGCTCCAAACCAGAC	ACCTTCGCCCACTTCACAACTTG
ARHGAP10	GCCTGATGCCACATTGCCTGAG	GACGGTCACCATCTTCCAGTTCAAG
MyoD1	CGCAACGCCATCCGCTATATCG	GTAGTAAGCACGGTCGTAGCAGTTC
Pax7	TGCCTAATCACATCCGCCACAAG	CTTCGTCCTCCTCCTCCTTCTTCC
MyoG	GCAAGAGGAAGTCGGTGTCTGTG	TGGAGGTGAGGGAGTGCAGATTG
GADPH	CACAGTCAAGGCAGAGAAC	TACTCAGCACCAGCATCA

Supplementary Table S6 Selection signals annotated to 23 candidate genes by top 20 interaction CNVs

CHR	POS		F_{ST}	V_{ST}	GENE
1	72849001 bp	72855000 bp	0.44936	0.637342927	ATP13A3
5	30425501 bp	30432500 bp	0.437353	0.659551295	KMT2D
7	89977001 bp	89982500 bp	0.434199	0.602733556	CELF5
8	9593001 bp	9601000 bp	0.689759	0.644452782	HMBOX1
11	98603501 bp	98606500 bp	0.437353	0.618546776	GLE1
11	105377001 bp	105389500 bp	0.490056	0.697100545	CACNA1B
13	53503001 bp	53514000 bp	0.437096	0.654978736	KCNQ2
14	15944001 bp	15949500 bp	0.456224	0.715165658	MATN2
15	42480001 bp	42485000 bp	0.526789	0.773314162	TEAD1
16	48856001 bp	48903000 bp	0.434199	0.631921431	PLCH2
17	60062001 bp	60297500 bp	0.918858	0.855420854	EDNRA
17	60301001 bp	61018500 bp	0.918858	0.877347065	ARHGAP10, PRMT9, NR3C2, TMEM184C
18	15272001 bp	15278000 bp	0.468566	0.67402736	ZC3H18
18	15290001 bp	15299500 bp	0.442146	0.680869415	CYBA
19	50673501 bp	50681000 bp	0.44936	0.61708302	BAHCC1
22	48097001 bp	48104000 bp	0.466683	0.635048801	PBRM1
22	49522501 bp	49527500 bp	0.444612	0.598522291	DOCK3
22	50571001 bp	50581500 bp	0.44936	0.67098526	RNF123
22	52556501 bp	52568000 bp	0.444612	0.635769213	NBEAL2
23	22410501 bp	22423000 bp	0.452638	0.64652245	VARS1

Supplementary Table S7 Kyoto Encyclopedia of Genes and Genomes (KEGG) analysis of candidate genes from top 20 CNV intersections between F_{ST} and V_{ST}

Term	Database	ID	Input number	Background number	P-Value	Corrected P-Value	Input
Cholinergic synapse	KEGG PATHWAY	hsa04725	2	112	0.002031132	0.049028275	CACNA1B KCNQ2
Calcium signaling pathway	KEGG PATHWAY	hsa04020	2	193	0.005795564	0.049028275	EDNRA CACNA1B
Terpenoid backbone biosynthesis	KEGG PATHWAY	hsa00900	1	22	0.013389154	0.050395287	MVD
Hippo signaling pathway - multiple species	KEGG PATHWAY	hsa04392	1	29	0.017429961	0.056087422	TEAD1
Nicotine addiction	KEGG PATHWAY	hsa05033	1	40	0.023747834	0.060146384	CACNA1B
Type II diabetes mellitus	KEGG PATHWAY	hsa04930	1	46	0.02717755	0.064271119	CACNA1B
Lysine degradation	KEGG PATHWAY	hsa00310	1	59	0.034569106	0.071140469	KMT2D
Aminoacyl-tRNA biosynthesis	KEGG PATHWAY	hsa00970	1	66	0.038526893	0.075113583	VARS1
Renin secretion	KEGG PATHWAY	hsa04924	1	69	0.040218332	0.076711787	EDNRA
Bacterial invasion of epithelial cells	KEGG PATHWAY	hsa05100	1	74	0.043031074	0.076711787	ARHGAP10
Inositol phosphate metabolism	KEGG PATHWAY	hsa00562	1	74	0.043031074	0.076711787	PLCH2
Leishmaniasis	KEGG PATHWAY	hsa05140	1	74	0.043031074	0.076711787	CYBA
Synaptic vesicle cycle	KEGG PATHWAY	hsa04721	1	78	0.04527559	0.078185139	CACNA1B
GABAergic synapse	KEGG PATHWAY	hsa04727	1	89	0.051422071	0.084971838	CACNA1B
Morphine addiction	KEGG PATHWAY	hsa05032	1	91	0.052535539	0.085252283	CACNA1B
Leukocyte transendothelial migration	KEGG PATHWAY	hsa04670	1	112	0.064151724	0.096050371	CYBA
Serotonergic synapse	KEGG PATHWAY	hsa04726	1	115	0.065800017	0.097441555	CACNA1B
Osteoclast differentiation	KEGG PATHWAY	hsa04380	1	128	0.072910585	0.105661864	CYBA
Dopaminergic synapse	KEGG PATHWAY	hsa04728	1	131	0.074544118	0.10688601	CACNA1B
Vascular smooth muscle contraction	KEGG PATHWAY	hsa04270	1	132	0.075088017	0.107099224	EDNRA
Fluid shear stress and atherosclerosis	KEGG PATHWAY	hsa05418	1	139	0.078886757	0.110197481	CYBA
Retrograde endocannabinoid signaling	KEGG PATHWAY	hsa04723	1	148	0.083748928	0.114626057	CACNA1B

Phagosome	KEGG PATHWAY	hsa04145	1	152	0.085902003	0.116397214	CYBA
Hippo signaling pathway	KEGG PATHWAY	hsa04390	1	154	0.086976725	0.117267127	TEAD1
Cushing syndrome	KEGG PATHWAY	hsa04934	1	155	0.087513633	0.117406904	KMT2D
cGMP-PKG signaling pathway	KEGG PATHWAY	hsa04022	1	167	0.093933015	0.122975107	EDNRA
Hepatocellular carcinoma	KEGG PATHWAY	hsa05225	1	168	0.094466009	0.12307831	PBRM1
NOD-like receptor signaling pathway	KEGG PATHWAY	hsa04621	1	178	0.099779483	0.128872195	CYBA
cAMP signaling pathway	KEGG PATHWAY	hsa04024	1	214	0.118662138	0.148190965	EDNRA
MAPK signaling pathway	KEGG PATHWAY	hsa04010	1	295	0.159772731	0.186631078	CACNA1B
Neuroactive ligand-receptor interaction	KEGG PATHWAY	hsa04080	1	338	0.180844949	0.207535743	EDNRA
Metabolic pathways	KEGG PATHWAY	hsa01100	2	1433	0.204685848	0.228271049	PLCH2|MVD
Pathways in cancer	KEGG PATHWAY	hsa05200	1	530	0.268921908	0.288054692	EDNRA

Supplementary Table S8 Gene Ontology (GO) analysis of candidate genes from top 20 CNV intersections between F_{ST} and V_{ST}

Term	Database	ID	Input number	Background number	P-Value	Corrected P-Value	Input
phosphatidylinositol phospholipase C activity	Gene Ontology	GO:0004435	2	26	0.000122906	0.033307477	PLCH2|EDNRA
regulation of blood pressure	Gene Ontology	GO:0008217	2	66	0.000730208	0.049028275	EDNRA|CACNA1B
tertiary granule membrane	Gene Ontology	GO:0070821	2	73	0.000887306	0.049028275	CYBA|NBEAL2
cellular_component	Gene Ontology	GO:0005575	3	433	0.002041117	0.049028275	PLCH2|VWA7|CELF5
regulation of ion transmembrane transport	Gene Ontology	GO:0034765	2	113	0.002066346	0.049028275	CACNA1B KCNQ2
protein binding	Gene Ontology	GO:0005515	14	11779	0.002105803	0.049028275	MATN2|NBE|KMT2D|CYBA|DOCK3|GLE1C|ACNA1B|AL2HVARS1|MBOX|KCNQ2|PBRM1|CELF5|EDNR|TEAD1
SH3 domain binding	Gene Ontology	GO:0017124	2	131	0.002749457	0.049028275	DOCK3|CYBA
DNA translocase activity	Gene Ontology	GO:0015616	1	5	0.003509482	0.049028275	PBRM1
response to hypoxia	Gene Ontology	GO:0001666	2	160	0.004042851	0.049028275	EDNRA|CYBA
positive regulation of mucus secretion	Gene Ontology	GO:0070257	1	6	0.004093249	0.049028275	CYBA
histone H3-K4 dimethylation	Gene Ontology	GO:0044648	1	6	0.004093249	0.049028275	KMT2D
regulation of telomerase activity	Gene Ontology	GO:0051972	1	6	0.004093249	0.049028275	HMBOX1
positive regulation of toll-like receptor 2 signaling pathway	Gene Ontology	GO:0034137	1	6	0.004093249	0.049028275	CYBA
positive regulation of defense response to bacterium	Gene Ontology	GO:1900426	1	6	0.004093249	0.049028275	CYBA
positive regulation of non-membrane spanning protein tyrosine kinase activity	Gene Ontology	GO:1903997	1	7	0.004676689	0.049028275	DOCK3
endothelin receptor signaling pathway	Gene Ontology	GO:0086100	1	7	0.004676689	0.049028275	EDNRA
positive regulation of NAD(P)H oxidase activity	Gene Ontology	GO:0033864	1	7	0.004676689	0.049028275	CYBA
regulation of translational termination	Gene Ontology	GO:0006449	1	7	0.004676689	0.049028275	GLE1
dolichyl diphosphate biosynthetic process	Gene Ontology	GO:0006489	1	7	0.004676689	0.049028275	MVD
biological_process	Gene Ontology	GO:0008150	3	594	0.004937499	0.049028275	PLCH2|VWA7|

							MATN2
hydrogen peroxide biosynthetic process	Gene Ontology	GO:0050665	1	8	0.005259803	0.049028275	CYBA
histone H3-K4 monomethylation	Gene Ontology	GO:0097692	1	8	0.005259803	0.049028275	KMT2D
regulation of glucose transmembrane transport	Gene Ontology	GO:0010827	1	9	0.005842589	0.049028275	EDNRA
isoprenoid biosynthetic process	Gene Ontology	GO:0008299	1	9	0.005842589	0.049028275	MVD
glial cell migration	Gene Ontology	GO:0008347	1	9	0.005842589	0.049028275	MATN2
double-stranded telomeric DNA binding	Gene Ontology	GO:0003691	1	9	0.005842589	0.049028275	HMBOX1
high voltage-gated calcium channel activity	Gene Ontology	GO:0008331	1	10	0.006425049	0.049028275	CACNA1B
artery smooth muscle contraction	Gene Ontology	GO:0014824	1	10	0.006425049	0.049028275	EDNRA
phosphatidylinositol metabolic process	Gene Ontology	GO:0046488	1	10	0.006425049	0.049028275	PLCH2
cellular response to angiotensin	Gene Ontology	GO:1904385	1	11	0.007007182	0.049028275	CYBA
aminoacyl-tRNA editing activity	Gene Ontology	GO:0002161	1	11	0.007007182	0.049028275	VARS1
positive regulation of intracellular estrogen receptor signaling pathway	Gene Ontology	GO:0033148	1	11	0.007007182	0.049028275	KMT2D
calcium ion binding	Gene Ontology	GO:0005509	3	693	0.007539839	0.049028275	PLCH2|MATN2 |CACNA1B|
head development	Gene Ontology	GO:0060322	1	12	0.007588989	0.049028275	EDNRA
NADPH oxidase complex	Gene Ontology	GO:0043020	1	12	0.007588989	0.049028275	CYBA
positive regulation of reactive oxygen species biosynthetic process	Gene Ontology	GO:1903428	1	12	0.007588989	0.049028275	CYBA
aminoacyl-tRNA metabolism involved in translational fidelity	Gene Ontology	GO:0106074	1	12	0.007588989	0.049028275	VARS1
respiratory burst	Gene Ontology	GO:0045730	1	13	0.00817047	0.049028275	CYBA
superoxide-generating NAD(P)H oxidase activity	Gene Ontology	GO:0016175	1	13	0.00817047	0.049028275	CYBA
MLL3/4 complex	Gene Ontology	GO:0044666	1	13	0.00817047	0.049028275	KMT2D
positive regulation of chromatin binding	Gene Ontology	GO:0035563	1	13	0.00817047	0.049028275	HMBOX1
nuclear membrane	Gene Ontology	GO:0031965	2	237	0.008579421	0.049028275	RNF123|GLE1
regulation of release of sequestered calcium ion into cytosol	Gene Ontology	GO:0051279	1	14	0.008751625	0.049028275	CYBA
response to amyloid-beta	Gene Ontology	GO:1904645	1	14	0.008751625	0.049028275	CACNA1B
pre-mRNA binding	Gene Ontology	GO:0036002	1	15	0.009332454	0.049028275	CELF5
enteric nervous system development	Gene Ontology	GO:0048484	1	15	0.009332454	0.049028275	EDNRA
node of Ranvier	Gene Ontology	GO:0033268	1	15	0.009332454	0.049028275	KCNQ2
chemical synaptic transmission	Gene Ontology	GO:0007268	2	248	0.009352542	0.049028275	CACNA1B|KC

ATP binding	Gene Ontology	GO:0005524	4	1463	0.009735448	0.049028275	NQ2 VARS1|MVD| CACNA1B| ATP13A3
superoxide anion generation	Gene Ontology	GO:0042554	1	16	0.009912958	0.049028275	CYBA
smooth muscle contraction	Gene Ontology	GO:0006939	1	16	0.009912958	0.049028275	EDNRA
vasoconstriction	Gene Ontology	GO:0042310	1	16	0.009912958	0.049028275	EDNRA
perinuclear endoplasmic reticulum	Gene Ontology	GO:0097038	1	17	0.010493136	0.049028275	CYBA
response to pain	Gene Ontology	GO:0048265	1	17	0.010493136	0.049028275	CACNA1B
histone methyltransferase activity (H3-K4 specific)	Gene Ontology	GO:0042800	1	17	0.010493136	0.049028275	KMT2D
axon initial segment	Gene Ontology	GO:0043194	1	17	0.010493136	0.049028275	KCNQ2
platelet formation	Gene Ontology	GO:0030220	1	19	0.011652518	0.050314094	NBEAL2
positive regulation of superoxide anion generation	Gene Ontology	GO:0032930	1	19	0.011652518	0.050314094	CYBA
ankyrin binding	Gene Ontology	GO:0030506	1	20	0.012231721	0.050314094	KCNQ2
superoxide metabolic process	Gene Ontology	GO:0006801	1	20	0.012231721	0.050314094	CYBA
poly(A)+ mRNA export from nucleus	Gene Ontology	GO:0016973	1	20	0.012231721	0.050314094	GLE1
histone H3-K4 trimethylation	Gene Ontology	GO:0080182	1	20	0.012231721	0.050314094	KMT2D
mRNA splice site selection	Gene Ontology	GO:0006376	1	21	0.0128106	0.050314094	CELF5
histone H3-K4 methylation	Gene Ontology	GO:0051568	1	21	0.0128106	0.050314094	KMT2D
Rac guanyl-nucleotide exchange factor activity	Gene Ontology	GO:0030676	1	21	0.0128106	0.050314094	DOCK3
translation initiation factor binding	Gene Ontology	GO:0031369	1	21	0.0128106	0.050314094	GLE1
neural crest cell development	Gene Ontology	GO:0014032	1	21	0.0128106	0.050314094	EDNRA
lysine-acetylated histone binding	Gene Ontology	GO:0070577	1	22	0.013389154	0.050395287	PBRM1
membrane depolarization	Gene Ontology	GO:0051899	1	22	0.013389154	0.050395287	CACNA1B
calcium ion import	Gene Ontology	GO:0070509	1	23	0.013967383	0.05185152	CACNA1B
telomeric DNA binding	Gene Ontology	GO:0042162	1	26	0.015700129	0.056087422	HMBOX1
voltage-gated calcium channel complex	Gene Ontology	GO:0005891	1	27	0.016277063	0.056087422	CACNA1B
hippo signaling	Gene Ontology	GO:0035329	1	27	0.016277063	0.056087422	TEAD1
regulation of calcium ion transport	Gene Ontology	GO:0051924	1	28	0.016853673	0.056087422	CACNA1B
regulation of translational initiation	Gene Ontology	GO:0006446	1	28	0.016853673	0.056087422	GLE1
proteolysis involved in cellular protein catabolic process	Gene Ontology	GO:0051603	1	28	0.016853673	0.056087422	RNF123
cation transport	Gene Ontology	GO:0006812	1	29	0.017429961	0.056087422	ATP13A3
beta-catenin-TCF complex assembly	Gene Ontology	GO:1904837	1	29	0.017429961	0.056087422	KMT2D
nuclear chromosome	Gene Ontology	GO:0000228	1	29	0.017429961	0.056087422	PBRM1
branching involved in blood vessel morphogenesis	Gene Ontology	GO:0001569	1	29	0.017429961	0.056087422	EDNRA

respiratory gaseous exchange by respiratory system	Gene Ontology	GO:0007585	1	30	0.018005925	0.056087422	EDNRA
response to axon injury	Gene Ontology	GO:0048678	1	30	0.018005925	0.056087422	MATN2
cellular response to gamma radiation	Gene Ontology	GO:0071480	1	30	0.018005925	0.056087422	CYBA
embryonic organ development	Gene Ontology	GO:0048568	1	31	0.018581566	0.056585652	TEAD1
oogenesis	Gene Ontology	GO:0048477	1	32	0.019156885	0.056585652	KMT2D
delayed rectifier potassium channel activity	Gene Ontology	GO:0005251	1	33	0.019731881	0.056585652	KCNQ2
response to interleukin-1	Gene Ontology	GO:0070555	1	33	0.019731881	0.056585652	CYBA
regulation of heart contraction	Gene Ontology	GO:0008016	1	33	0.019731881	0.056585652	CACNA1B
histone methyltransferase complex	Gene Ontology	GO:0035097	1	33	0.019731881	0.056585652	KMT2D
activation of phospholipase C activity	Gene Ontology	GO:0007202	1	34	0.020306555	0.056585652	EDNRA
positive regulation of telomerase activity	Gene Ontology	GO:0051973	1	34	0.020306555	0.056585652	HMBOX1
ATP-dependent chromatin remodeling	Gene Ontology	GO:0043044	1	34	0.020306555	0.056585652	PBRM1
positive regulation of telomere maintenance via telomerase	Gene Ontology	GO:0032212	1	34	0.020306555	0.056585652	HMBOX1
neuronal cell body	Gene Ontology	GO:0043025	2	376	0.020462708	0.056585652	CACNA1B|CYBA
regulation of cholesterol biosynthetic process	Gene Ontology	GO:0045540	1	35	0.020880906	0.057158843	MVD
tRNA aminoacylation for protein translation	Gene Ontology	GO:0006418	1	37	0.022028642	0.059697621	VARS1
voltage-gated calcium channel activity	Gene Ontology	GO:0005245	1	38	0.022602028	0.060146384	CACNA1B
cytosol	Gene Ontology	GO:0005829	7	5095	0.022971139	0.060146384	HMBOX1|DOCK3|VARS1|MVD|RNF123|NBEAL2|GLE1
cholesterol biosynthetic process	Gene Ontology	GO:0006695	1	40	0.023747834	0.060146384	MVD
activation of adenylate cyclase activity	Gene Ontology	GO:0007190	1	40	0.023747834	0.060146384	EDNRA
chromatin silencing	Gene Ontology	GO:0006342	1	40	0.023747834	0.060146384	KMT2D
positive regulation of pri-miRNA transcription by RNA polymerase II	Gene Ontology	GO:1902895	1	40	0.023747834	0.060146384	TEAD1
response to nutrient levels	Gene Ontology	GO:0031667	1	41	0.024320256	0.061025827	CYBA
Hsp70 protein binding	Gene Ontology	GO:0030544	1	42	0.024892356	0.061881256	MVD
dendrite	Gene Ontology	GO:0030425	2	420	0.025117853	0.061881256	CACNA1B|CYBA

cellular response to organic cyclic compound	Gene Ontology	GO:0071407	1	45	0.026606732	0.063809066	CYBA
regulation of megakaryocyte differentiation	Gene Ontology	GO:0045652	1	45	0.026606732	0.063809066	KMT2D
positive regulation of phagocytosis	Gene Ontology	GO:0050766	1	45	0.026606732	0.063809066	CYBA
chromatin binding	Gene Ontology	GO:0003682	2	443	0.027708314	0.064271119	BAHCC1|PBRM1
response to activity	Gene Ontology	GO:0014823	1	47	0.027748048	0.064271119	CYBA
inositol phosphate metabolic process	Gene Ontology	GO:0043647	1	47	0.027748048	0.064271119	PLCH2
positive regulation of tumor necrosis factor production	Gene Ontology	GO:0032760	1	50	0.029457621	0.067652672	CYBA
neurotransmitter secretion	Gene Ontology	GO:0007269	1	51	0.03002684	0.06838045	CACNA1B
membrane	Gene Ontology	GO:0016020	4	2075	0.030983841	0.069797772	ATP13A3|CYBA|NBEAL2|GLE1
Cajal body	Gene Ontology	GO:0015030	1	53	0.031164319	0.069797772	HMBOX1
cis-regulatory region sequence-specific DNA binding	Gene Ontology	GO:0000987	1	55	0.032300522	0.070671187	TEAD1
phosphatidylinositol-mediated signaling	Gene Ontology	GO:0048015	1	55	0.032300522	0.070671187	PLCH2
neutrophil degranulation	Gene Ontology	GO:0043312	2	482	0.032336631	0.070671187	CYBA|NBEAL2
DNA binding	Gene Ontology	GO:0003677	3	1209	0.032793711	0.071096765	TEAD1|KMT2D|PBRM1
positive regulation of smooth muscle cell proliferation	Gene Ontology	GO:0048661	1	58	0.034002438	0.071140469	CYBA
cell redox homeostasis	Gene Ontology	GO:0045454	1	59	0.034569106	0.071140469	CYBA
positive regulation of cell population proliferation	Gene Ontology	GO:0008284	2	501	0.034695287	0.071140469	MVD|KMT2D
cellular response to glucose stimulus	Gene Ontology	GO:0071333	1	60	0.035135457	0.071140469	CYBA
voltage-gated potassium channel activity	Gene Ontology	GO:0005249	1	60	0.035135457	0.071140469	KCNQ2
modulation of chemical synaptic transmission	Gene Ontology	GO:0050804	1	60	0.035135457	0.071140469	CACNA1B
adenylate cyclase-inhibiting G protein-coupled receptor signaling pathway	Gene Ontology	GO:0007193	1	60	0.035135457	0.071140469	EDNRA
centrosome	Gene Ontology	GO:0005813	2	506	0.035326991	0.071140469	HMBOX1|GLE1
ficolin-1-rich granule membrane	Gene Ontology	GO:0101003	1	61	0.03570149	0.071140469	NBEAL2
response to estrogen	Gene Ontology	GO:0043627	1	61	0.03570149	0.071140469	KMT2D
nuclear pore	Gene Ontology	GO:0005643	1	63	0.036832603	0.072858652	GLE1
vascular endothelial growth factor receptor signaling pathway	Gene Ontology	GO:0048010	1	64	0.037397683	0.073440378	CYBA

electron transport chain	Gene Ontology	GO:0022900	1	69	0.040218332	0.076711787	CYBA
stress fiber	Gene Ontology	GO:0001725	1	69	0.040218332	0.076711787	CYBA
sequence-specific double-stranded DNA binding	Gene Ontology	GO:1990837	2	553	0.04148235	0.076711787	TEAD1|HMBOX1
positive regulation of transcription, DNA-templated	Gene Ontology	GO:0045893	2	556	0.041888267	0.076711787	TEAD1|HMBOX1
positive regulation of endothelial cell proliferation	Gene Ontology	GO:0001938	1	73	0.042469158	0.076711787	CYBA
metal ion binding	Gene Ontology	GO:0046872	4	2298	0.04271388	0.076711787	ATP13A3|CYBA|RNF123|KMT2D
phagocytic vesicle membrane	Gene Ontology	GO:0030670	1	74	0.043031074	0.076711787	CYBA
electron transfer activity	Gene Ontology	GO:0009055	1	74	0.043031074	0.076711787	CYBA
antigen processing and presentation of exogenous peptide antigen via MHC class I, TAP-dependent	Gene Ontology	GO:0002479	1	75	0.043592676	0.076711787	CYBA
calcium ion transport	Gene Ontology	GO:0006816	1	75	0.043592676	0.076711787	CACNA1B
regulation of alternative mRNA splicing, via spliceosome	Gene Ontology	GO:0000381	1	75	0.043592676	0.076711787	CELF5
protein localization	Gene Ontology	GO:0008104	1	77	0.044714933	0.078179012	NBEAL2
cellular response to mechanical stimulus	Gene Ontology	GO:0071260	1	79	0.045835931	0.078185139	CYBA
lipid catabolic process	Gene Ontology	GO:0016042	1	79	0.045835931	0.078185139	PLCH2
plasma membrane	Gene Ontology	GO:0005886	6	4619	0.045872461	0.078185139	CACNA1B|KCNQ2|PLCH2|CYBA|EDNRA|NBEAL2
amyloid-beta binding	Gene Ontology	GO:0001540	1	80	0.046395958	0.078583154	CACNA1B
positive regulation of cell growth	Gene Ontology	GO:0030307	1	81	0.04695567	0.079037184	CYBA
locomotory behavior	Gene Ontology	GO:0007626	1	85	0.04919138	0.081784441	CACNA1B
voltage-gated potassium channel complex	Gene Ontology	GO:0008076	1	85	0.04919138	0.081784441	KCNQ2
positive regulation of interleukin-6 production	Gene Ontology	GO:0032755	1	90	0.051978962	0.085252283	CYBA
specific granule membrane	Gene Ontology	GO:0035579	1	91	0.052535539	0.085252283	CYBA
secretory granule	Gene Ontology	GO:0030141	1	92	0.053091804	0.085642137	CYBA
basement membrane	Gene Ontology	GO:0005604	1	93	0.053647757	0.086026877	MATN2
small GTPase mediated signal transduction	Gene Ontology	GO:0007264	1	94	0.054203397	0.086406592	DOCK3
cellular response to oxidative stress	Gene Ontology	GO:0034599	1	95	0.054758726	0.086781373	CYBA
cellular calcium ion homeostasis	Gene Ontology	GO:0006874	1	98	0.05642284	0.088898777	ATP13A3
mRNA export from nucleus	Gene Ontology	GO:0006406	1	101	0.058084152	0.090464398	GLE1
PML body	Gene Ontology	GO:0016605	1	101	0.058084152	0.090464398	HMBOX1
chromatin remodeling	Gene Ontology	GO:0006338	1	102	0.058637301	0.090804048	PBRM1

peroxisome	Gene Ontology	GO:0005777	1	108	0.061949673	0.094927261	MVD
phospholipid binding	Gene Ontology	GO:0005543	1	109	0.06250065	0.094927261	GLE1
presynapse	Gene Ontology	GO:0098793	1	109	0.06250065	0.094927261	CACNA1B
nuclear chromosome, telomeric region	Gene Ontology	GO:0000784	1	110	0.063051317	0.094927261	HMBOX1
neuron migration	Gene Ontology	GO:0001764	1	110	0.063051317	0.094927261	MATN2
calcium ion transmembrane transport	Gene Ontology	GO:0070588	1	115	0.065800017	0.097441555	CACNA1B
molecular_function	Gene Ontology	GO:0003674	2	742	0.069802964	0.102806998	PLCH2|VWA7
potassium ion transmembrane transport	Gene Ontology	GO:0071805	1	123	0.070181899	0.102806998	KCNQ2
cellular response to tumor necrosis factor	Gene Ontology	GO:0071356	1	125	0.071274294	0.10384588	CYBA
protein-containing complex assembly	Gene Ontology	GO:0065003	1	129	0.073455402	0.105885181	TEAD1
mitotic cell cycle	Gene Ontology	GO:0000278	1	134	0.076174898	0.108080614	PBRM1
heme binding	Gene Ontology	GO:0020037	1	135	0.07671788	0.108284091	CYBA
extracellular matrix structural constituent	Gene Ontology	GO:0005201	1	137	0.077802929	0.109246599	MATN2
cell population proliferation	Gene Ontology	GO:0008283	1	142	0.080510216	0.111888557	EDNRA
centriole	Gene Ontology	GO:0005814	1	144	0.081591002	0.112812048	GLE1
positive regulation of cytosolic calcium ion concentration	Gene Ontology	GO:0007204	1	146	0.082670572	0.113724492	EDNRA
ciliary basal body	Gene Ontology	GO:0036064	1	151	0.085364188	0.116249724	GLE1
ribonucleoprotein complex	Gene Ontology	GO:1990904	1	156	0.088050239	0.1175449	CELF5
transcription initiation from RNA polymerase II promoter	Gene Ontology	GO:0006367	1	160	0.090193645	0.119816067	TEAD1
histone binding	Gene Ontology	GO:0042393	1	163	0.091798036	0.121352526	KMT2D
DNA-binding transcription factor activity, RNA polymerase II-specific	Gene Ontology	GO:0000981	2	874	0.092436856	0.121603826	TEAD1|HMBOX1
nuclear chromatin	Gene Ontology	GO:0000790	2	915	0.099864062	0.128872195	TEAD1|HMBOX1
nuclear envelope	Gene Ontology	GO:0005635	1	182	0.101896511	0.130871822	GLE1
protein C-terminus binding	Gene Ontology	GO:0008022	1	189	0.105589856	0.134342024	CACNA1B
heart development	Gene Ontology	GO:0007507	1	189	0.105589856	0.134342024	EDNRA
mRNA binding	Gene Ontology	GO:0003729	1	200	0.111364347	0.140370875	CELF5
calmodulin binding	Gene Ontology	GO:0005516	1	200	0.111364347	0.140370875	KCNQ2
in utero embryonic development	Gene Ontology	GO:0001701	1	202	0.112410416	0.141033439	EDNRA
axon guidance	Gene Ontology	GO:0007411	1	222	0.122806529	0.152663162	MATN2
transcription regulator complex	Gene Ontology	GO:0005667	1	226	0.124871728	0.154521636	TEAD1
cytoplasm	Gene Ontology	GO:0005737	5	4624	0.126144268	0.155018835	PLCH2|CELF5|HMBOX1|RNF123|GLE1

ATPase activity	Gene Ontology	GO:0016887	1	229	0.126417574	0.155018835	ATP13A3
extracellular matrix	Gene Ontology	GO:0031012	1	233	0.128474639	0.156128373	MATN2
ubiquitin-protein transferase activity	Gene Ontology	GO:0004842	1	233	0.128474639	0.156128373	RNF123
transcription coactivator activity	Gene Ontology	GO:0003713	1	248	0.136147447	0.164714098	KMT2D
DNA-binding transcription repressor activity, RNA polymerase II-specific	Gene Ontology	GO:0001227	1	253	0.138690659	0.167045194	HMBOX1
protein deubiquitination	Gene Ontology	GO:0016579	1	262	0.143250405	0.171620141	RNF123
transcription regulatory region sequence-specific DNA binding	Gene Ontology	GO:0000976	1	263	0.143755616	0.171620141	KMT2D
positive regulation of transcription by RNA polymerase II	Gene Ontology	GO:0045944	2	1159	0.147155678	0.174908723	TEAD1|KMT2D
response to drug	Gene Ontology	GO:0042493	1	280	0.152300724	0.180233608	CYBA
nucleoplasm	Gene Ontology	GO:0005654	4	3630	0.158271713	0.186274508	HMBOX1|TEAD1|KMT2D|PBRM1
endosome	Gene Ontology	GO:0005768	1	293	0.158780116	0.186274508	CYBA
protein heterodimerization activity	Gene Ontology	GO:0046982	1	297	0.160764226	0.186983284	CYBA
nervous system development	Gene Ontology	GO:0007399	1	305	0.164719025	0.190764341	KCNQ2
nuclear body	Gene Ontology	GO:0016604	1	307	0.165704936	0.191089522	HMBOX1
nucleus	Gene Ontology	GO:0005634	5	5208	0.181498049	0.207535743	HMBOX1|TEAD1|CYBA|CELF5|KMT2D
protein-containing complex binding	Gene Ontology	GO:0044877	1	349	0.186153763	0.211965	HMBOX1
apical plasma membrane	Gene Ontology	GO:0016324	1	354	0.188555967	0.213801954	CYBA
integral component of plasma membrane	Gene Ontology	GO:0005887	2	1380	0.193307833	0.218276761	EDNRA|KCNQ2
collagen-containing extracellular matrix	Gene Ontology	GO:0062023	1	370	0.196197526	0.220620454	MATN2
inflammatory response	Gene Ontology	GO:0006954	1	381	0.201411117	0.22554716	CYBA
negative regulation of cell population proliferation	Gene Ontology	GO:0008285	1	394	0.207530934	0.230495423	PBRM1
identical protein binding	Gene Ontology	GO:0042802	2	1456	0.209651123	0.231899814	HMBOX1|GLE1
sequence-specific DNA binding	Gene Ontology	GO:0043565	1	405	0.212674179	0.234287408	HMBOX1
focal adhesion	Gene Ontology	GO:0005925	1	418	0.218711398	0.239962708	CYBA
synapse	Gene Ontology	GO:0045202	1	420	0.219636261	0.240005753	KCNQ2
protein kinase binding	Gene Ontology	GO:0019901	1	461	0.238366784	0.259427304	NBEAL2
DNA-binding transcription activator activity, RNA polymerase II-specific	Gene Ontology	GO:0001228	1	466	0.240621354	0.260833547	TEAD1
protein ubiquitination	Gene Ontology	GO:0016567	1	486	0.249575957	0.269462487	RNF123
oxidation-reduction process	Gene Ontology	GO:0055114	1	525	0.26674777	0.286859705	CYBA

negative regulation of transcription, DNA-templated	Gene Ontology	GO:0045892	1	536	0.271522735	0.289695517	HMBOX1
innate immune response	Gene Ontology	GO:0045087	1	558	0.280983588	0.298613931	CYBA
DNA-binding transcription factor activity	Gene Ontology	GO:0003700	1	607	0.301634906	0.319308826	TEAD1
RNA polymerase II cis-regulatory region sequence-specific DNA binding	Gene Ontology	GO:0000978	1	656	0.321718162	0.339243665	TEAD1
protein homodimerization activity	Gene Ontology	GO:0042803	1	660	0.323332993	0.339624965	MVD
regulation of transcription, DNA-templated	Gene Ontology	GO:0006355	1	773	0.367462073	0.384487343	KMT2D
negative regulation of transcription by RNA polymerase II	Gene Ontology	GO:0000122	1	832	0.389395237	0.405869651	HMBOX1
nucleolus	Gene Ontology	GO:0005730	1	839	0.391948671	0.406965862	GLE1
endoplasmic reticulum membrane	Gene Ontology	GO:0005789	1	942	0.428359975	0.44307463	CYBA
Golgi apparatus	Gene Ontology	GO:0005794	1	1002	0.448599102	0.462244702	CYBA
signal transduction	Gene Ontology	GO:0007165	1	1013	0.452234479	0.464155846	EDNRA
endoplasmic reticulum	Gene Ontology	GO:0005783	1	1018	0.453879333	0.464155846	NBEAL2
G protein-coupled receptor signaling pathway	Gene Ontology	GO:0007186	1	1132	0.490125202	0.499338082	EDNRA
mitochondrion	Gene Ontology	GO:0005739	1	1258	0.527507347	0.535410079	VARS1
RNA binding	Gene Ontology	GO:0003723	1	1366	0.557449081	0.563689182	CELF5
extracellular space	Gene Ontology	GO:0005615	1	1572	0.609602731	0.614135093	GLE1
integral component of membrane	Gene Ontology	GO:0016021	2	3643	0.643320256	0.645702924	ATP13A3|KCNQ2
extracellular region	Gene Ontology	GO:0005576	1	1843	0.669316716	0.669316716	VWA7